

BUCKLING OF RIBBED PLATES

A THESIS

Presented to

The Faculty of the Division of Graduate
Studies and Research

by

Dieter Bounin

In Partial Fulfillment


of the Requirements for the Degree
Master of Science in Civil Engineering

Georgia Institute of Technology

December, 1971

BUCKLING OF RIBBED PLATES

Approved:


Chairman

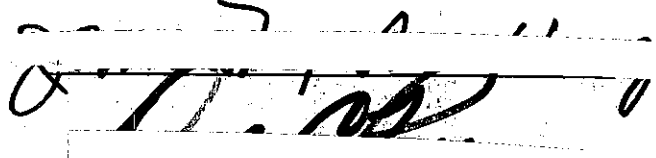

Date Approved by Chairman: 9/30/71

TABLE OF CONTENTS

	Page
ACKNOWLEDGMENTS	iv
LIST OF ILLUSTRATIONS	v
NOTATIONS	vi
SUMMARY	ix
Chapter	
I. INTRODUCTION	1
Buckling Modes	
Review of Literature	
Buckling of Flat Plates	
Buckling of Ribbed Plates	
Closed Form Field or Functional Approach	
to Ribbed Plates	
Summary of Literature	
Purpose of Investigation	
II. NON-COMPOSITE FLEXURAL ANALYSIS	17
Derivation of Boundary Force-Deformation Relations	
Governing Differential Equation	
Flexural Stiffness Matrix	
Derivation of the Buckling Criteria	
Equilibrium Equations	
Displacements	
Governing Difference Equations for the	
Rib Line Deformations	
Simple Side Supports	
Buckling with Simple Side Supports	
Numerical Examples for Simple Side Supports	
Boundary Deflections	
Rib Boundaries	
Buckling with Rib Boundaries	
Numerical Examples for Rib Boundaries	
III. COMPOSITE MEMBRANE ANALYSIS	50
Derivation of Boundary Force-Deformation Relations	
Governing Differential Equation	
Solution for Symmetric Case	
Solution for Anti-Symmetric Case	
Stiffness Matrix	

Chapter	Page
III. Continued	
Derivation of the Buckling Criteria	
Equilibrium Equations	
Displacements	
Governing Difference Equations for the	
Rib Line Displacements	
Simple Side Supports	
Buckling with Simple Side Supports	
Boundary Deflections	
Rib Boundary	
Buckling with Rib Boundaries	
IV. CONCLUSIONS	74
APPENDIX	76
BIBLIOGRAPHY	83

ACKNOWLEDGMENTS

My special appreciation is extended to Dr. Richard R. Avent, the Chairman of my thesis committee, for his invaluable advice, guidance, encouragement, and patience in completing this thesis.

I would like to thank the members of my thesis committee, Dr. Dale C. Perry and Dr. James T. Wang, for reading and criticizing this thesis and for their helpful and knowledgeable suggestions and corrections.

Also, I wish to extend appreciation to the School of Civil Engineering for the research assistantship received during my graduate studies.

LIST OF ILLUSTRATIONS

	Page
1. Cable Stayed Bridge.	1
2. Plate with I-Beam Stiffeners	2
3. Plate with Flat Strip Stiffeners	2
4. Local Buckling Mode of a Ribbed Plate.	3
5. Symmetric and Anti-Symmetric Buckling Modes.	4
6. Flat Plate in Compression.	5
7. Panel with Boundary Forces and Deformations for the Non-Composite Flexural Analysis.	17
8. Non-Composite Flexural Model	27
9. Applied Rib Line and Fixed Edge Panel Forces and Moments . . .	29
10. Curves for k_{cr} for Simple Side Supports.	41
11. Plate with Rib Boundaries.	44
12. Curves for k_{cr} for Rib Boundaries Symmetric Boundary Deflections.	49
13. Panel with Boundary Forces and Deformations for the Composite Membrane Analysis.	50
14. Composite Membrane Model	63
15. Beam Element with Applied Lateral Loads and Moments and Axial Force.	77
16. Transformation of the W-Axis of the Beam	79
17. Beam Element with Applied Loads and Axial Force.	80



LIST OF NOTATIONS

$A_i - D_i$	Constants in solution to panel equations
a, \bar{a}, \bar{a}^b, b	Panel width, rib depth, boundary rib depth, panel length
B, B'	Rib flexural rigidity about major and minor axes
$b_{11} - b_{24}$	Membrane stiffness coefficients
C_{ik}, C'_{ik}	Coefficient determinants
$\bar{c}_{11} - \bar{c}_{22}$	Modified membrane stiffness coefficients
D, \bar{D}_x, \bar{D}_y	Flexural plate rigidity and differential operators
$d_{11} - d_{24}$	Plate stiffness coefficients
E	Young's modulus
e	Eccentricity of forces on ribs
$\bar{e}_{11} - \bar{e}_{22}$	Modified plate stiffness coefficients
F_i	Membrane stress function
H	Axial force resultant of rib
I_i, I_i', J_i	Constants in plate solution
$I^s - J^{a/s}$	Constants in membrane solution
i, k	Summation indices in infinite and finite series
\bar{k}	Ratio between torsional and lateral bending stiffness of rib
k_{cr}	Buckling coefficient
l	Plate width
$M, \bar{M}, M_i, \bar{M}_i$	Panel edge flexural and rib torsional moments and coefficients
M^a, M^f	Applied and fixed edge panel moments
M^e, M_i^e	Equivalent rib line moments and coefficients
M_{ik}^φ	Weighted coefficient of double series for M^e

LIST OF NOTATIONS (Continued)

m_x, m_{xy}, m_y	Interior panel moments
$m_1 - m_4$	Roots of characteristic equation
N, \bar{N}	Panel edge direct force resultants and transverse rib loads
$N_i, N_i^s, N_i^{a/s}$	Coefficients of panel edge force resultants
n	Discrete coordinate of terminal rib line
$\bar{n}_x, \bar{n}_{xy}, \bar{n}_y$	Interior membrane forces in basic state
n_x, n_{xy}, n_y	Additional membrane forces in deformed state
N, N_y, P	Applied longitudinal compressive stress resultants on panel ends and on ribs
P^a, P^e, P_i, P_{ik}	Applied and equivalent transverse rib line loads and coefficients
$P_i^s, P_i^{a/s}$	Coefficients of boundary rib loading
Q_x, q	Interior panel shear and transverse load
r	Discrete coordinate to designate rib line
r	Radius of gyration of ribs
S^f, S, S_i	Fixed and other panel edge flexural shear resultants and coefficients
$s_i^s, s_i^{a/s}, \bar{s}_i^s, \bar{s}_i^{a/s}$	Coefficients of flexural shear at boundary for simple side supports and for imposed deflections
$T, T_i, T_i^s, T_i^{a/s}$	Panel edge membrane shear resultants and coefficients
t, \bar{t}, \bar{t}^b	Panel thickness, interior and boundary rib thickness
$t_i^s, t_i^{a/s}, \bar{t}_i^s, \bar{t}_i^{a/s}$	Coefficients of membrane shear at boundary
$U, U_i, \bar{U}_i, U_{ik}$	Rib line displacements and coefficients
$V - V_{ik}$	Rib line displacements and coefficients
$W - W_{ik}$	Rib line displacements and coefficients

LIST OF NOTATIONS (Continued)

$V_i^s, V_i^{a/s}, W_i^s, W_i^{a/s}$	Coefficients of imposed boundary displacements
\bar{u}, \bar{v}	Membrane displacements in basic state
u, v, w	Continuous variable displacements
x, y, z	Continuous variable coordinates
α_i	Principal parameter
β, λ	Plate and membrane aspect ratios
γ, δ	Ratios of rib stiffness and area to plate rigidity and area
$\gamma_i - \bar{\gamma}_i'$	Parameters in governing equations for ribbed plate
$\bar{\gamma}_i^b, \bar{\gamma}_i'^b, \epsilon_i^b - \bar{\epsilon}_i'^b$	Parameters for boundary deflections
ϵ	Applied longitudinal strain
ζ, ξ	Arguments of plate solution functions
$\theta - \theta_{ik}$	Rib line rotations and coefficients
ν, π	Poisson's ratio and standard ratio
σ	Applied longitudinal stress
σ_k	$1 - \cos \frac{k\pi}{n}$
σ_{cr}	Buckling stress
φ_k, φ_r	Cosine weighting function
φ, Φ	Parameters in membrane solution
 r	Second central difference operator
 r	Mean difference operator
Δ_r	First forward difference operator
∇_r	First backward difference operator

SUMMARY

Closed form solutions are presented for the elastic analysis of deflections and initial buckling of rectangular ribbed plates. The plates are subjected to uniform compressive stress along the two simply supported ends and are stiffened by uniform and equidistant ribs. The techniques used permit the realistic treatment of plates having simple side supports and of those having boundary beams with flexural and torsional rigidity. The solutions employed are double Fourier series which are infinite with respect to the continuous variable along the rib line and finite with respect to the discrete variable denoting the ribs. Simple algebraic corrective terms are added where required by the boundary conditions.

The results are based on two rationally formulated discrete-continuous models of the fourth order. The only assumptions made are those associated with flexural and membrane plate theory and classical beam theory. In the Non-Composite Flexural Model, the structure is proportioned so that the effects of the in-plane deformations and the T-beam action can be neglected in determining the stiffness matrices of the elements. In the Composite Membrane Model, the effects of the out-of-plane deformations are neglected.

The formulas developed are improvements over those based on orthotropic plate theory in that the assumptions of an equivalent continuum are avoided. Another major improvement is the independence of the form of the solution with respect to the stability criteria of the number of ribs. A few results are numerically illustrated and compared with existing theories.

CHAPTER I

INTRODUCTION

Structural ribbed plates have been used for many years in the construction of orthotropic bridge decks, floor systems, airplanes and ship hulls. They are structurally efficient and functional in that the increase in plate stability by adding longitudinal ribs is much more economical than by increasing the plate thickness. The purpose of this thesis is to present efficient methods of investigating the stability of ribbed plates subjected to axial loads. There are various ways in which an axially loaded ribbed plate is utilized, one of which is shown in Figure 1. At points of concentrated compressive loads in a cable stayed bridge, ribs can sustain these loads which are then distributed over the whole cross section of the rib-plate system. The typical ribbed plate is an all steel orthotropic bridge deck with angles, I-beams or narrow plates welded to the deck panels (Figures 2 and 3). However, a ribbed plate may also be of composite design, consisting of steel beams and a concrete slab.

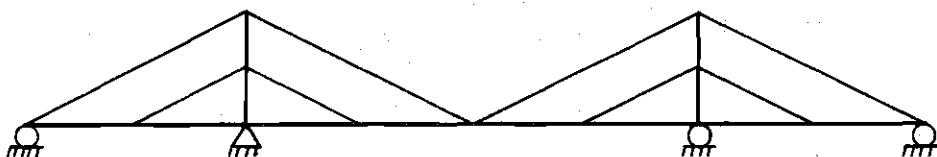


Figure 1. Cable Stayed Bridge.

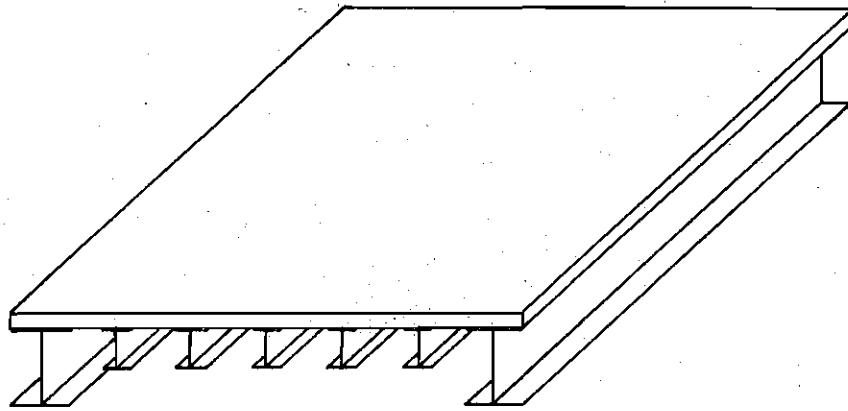


Figure 2. Plate with I-Beam Stiffeners

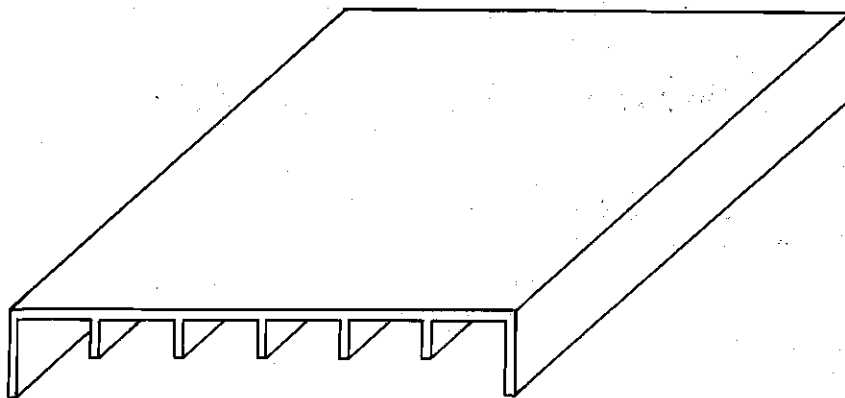


Figure 3. Plate with Flat Strip Stiffeners

1. Buckling Modes

In the course of an investigation of ribbed plates in compression, two major modes of buckling have to be considered. The first is local buckling of the plate. In this case, certain longitudinal and transverse elements of the structure, the nodal lines, remain straight and undeflected. All ribs coincide with the longitudinal nodal lines. They remain unbuckled and are subjected to torsion in addition to axial compression (Figure 4).



Figure 4. Local Buckling Mode of a Ribbed Plate.

For zero torsional rigidity of the ribs, the nodal lines coincide with the lines of inflexion of the buckled surface. Each panel then is subjected to zero boundary moments and can, therefore, be considered as being simply supported. In the longitudinal direction, the buckling also occurs in sinusoidal waves. The number of half waves, however, is one of the unknowns of the problem.

The second buckling mode is called system buckling. It can occur

in any number of half waves in the lateral direction, except that which is equal to the number of panels which, here, has been called local buckling. For an odd number of half waves, the buckling occurs in the symmetric mode and in an anti-symmetric mode for an even number. Both the plate and the stiffeners undergo lateral deflections as shown in Figure 5.

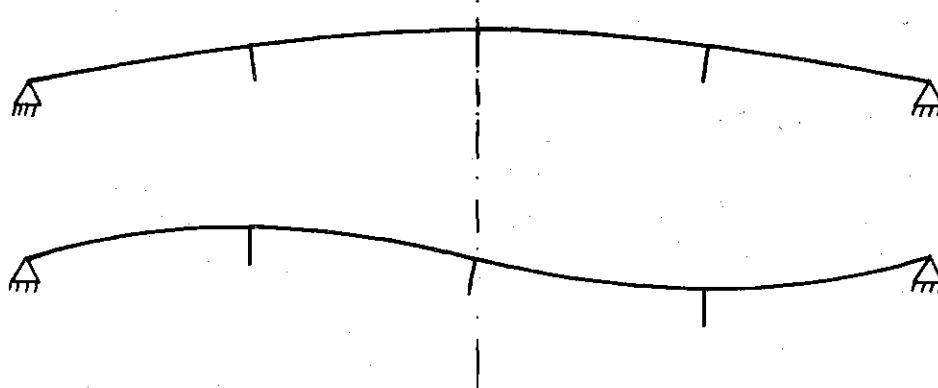


Figure 5. Symmetric and Anti-Symmetric Buckling Modes

In their respective vertical planes, the ribs are subjected to bending of varying degree, depending on their location in the system. They are also subjected to torsion about their longitudinal axis. For deep beam type ribs, ordinary beam theory becomes inadequate and membrane analysis is necessary. The plate itself is subjected to bending moments and shear forces if a Non-Composite Flexural Model (Chapter II) is used in the analysis. For the Composite Membrane Model (Chapter III), the plate is subjected to direct tensile or compressive forces.

Numbers of half waves greater than the number of panels are not investigated in this thesis. Since the main interest here is in the

initial buckling of bridge type structures with length to width ratios equal to or larger than one, that latter case would not lead to the lowest buckling stresses.

2. Review of Literature

2.1. Buckling of Flat Plates

Many classic reference texts, such as Timoshenko [1] and Girkmann [2], treat the buckling of unstiffened, simply supported plates compressed in one direction (Figure 6).

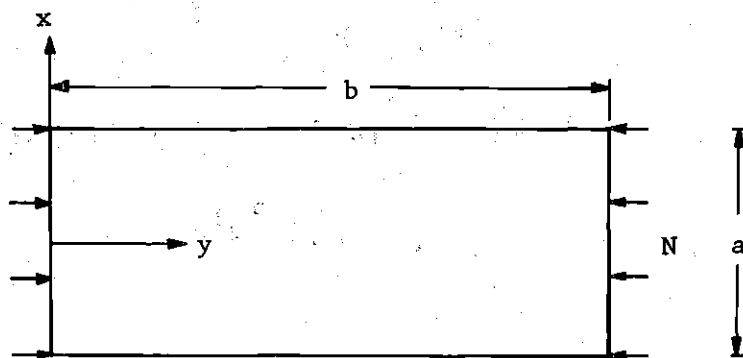


Figure 6. Flat Plate in Compression.

The first successful investigation in this field was published by Bryan [3]. The approach used by Timoshenko was to assume a sine variation of the deflection surface in both directions. Using the potential energy theorem, a minimum was found for one half-wave sine variation in the transverse direction. The one term solution of the minimum potential energy theorem is exact for the case of simple supports on all four sides. The final results for the buckling loads was found to be

$$N_{cr} = \sigma_{cr} t = \frac{\pi^2 D}{a^2} \left(\frac{ib}{a} + \frac{a}{ib} \right)^2 = k_{cr} \frac{\pi^2 D}{a^2} \quad (1)$$

or

$$\sigma_{cr} = k_{cr} \frac{\pi^2 E t^2}{12(1-\nu^2) a^2}$$

where $D = \frac{Et^3}{12(1-\nu^2)}$ is the plate stiffness and i is the number of half-waves in the longitudinal direction into which the plate buckles. This number of half-waves depends only on the ratio $\frac{b}{a}$ and not on the plate properties. The only unknown in Eq. (1) is i . For sufficiently short plates and small values of $\frac{b}{a}$, buckling occurs in one half-wave. Above a certain ratio of $\frac{b}{a}$, two half-waves are formed. For the limiting ratio, both cases are equally possible, having the same buckling load

$N_{cr} = t \cdot \sigma_{cr}$. Eq. (1) must yield the same N_{cr} whether $i = 1$ or $i = 2$ is introduced. In the same way, it is possible to determine the limiting ratio for buckling into i or $i + 1$ half-waves. The limiting ratio can be found from the equation

$$\frac{ib}{a} - \frac{a}{ib} = \frac{(i+1)b}{a} - \frac{a}{(i+1)b}$$

which yields

$$\frac{b}{a} = \sqrt{i(i+1)}$$

For $i = 1, 2, 3, \dots$ the ratios are $\frac{b}{a} = \sqrt{2}, \sqrt{6}, \sqrt{12}, \dots$

or $b = 1.414a, 2.449a, 3.464a, \dots$

Solving the governing differential equation of the plate in compression, Bleich [8] obtained the same solution as did Timoshenko with the potential energy approach. The solution to the differential equation also provides results for plates with arbitrary side boundary conditions. The general solution used for inhomogeneous boundary conditions is the Levy assumption of a sine variation only in the longitudinal direction and a particular solution in the transverse direction that has to satisfy the boundary conditions. Each boundary condition provides one equation for a system of simultaneous homogeneous equations in terms of the coefficients of the Levy solution. Non-trivial solutions exist only for the determinant of coefficients being equal to zero. Therefore, $\det = 0$ is the buckling criterion which leads to the stability condition. All conceivable modes of buckling are contained within this criterion. The various possibilities are represented by the successive roots of the determinant. The elements of this stability determinant are transcendental functions of the longitudinal compressive stress and the longitudinal half wave length, $\frac{b}{i}$. For assumed values of i there are, in general, an infinite number of roots to $\det = 0$, of which, however, only the first and smallest is relevant. The correct value of i is the one which minimizes the critical stress, and can be found by investigating the range of $i = 1$ to i equal to the first integer larger than the ratio $\frac{b}{a}$.

2.2. Buckling of Ribbed Plates

The discussion on this topic was opened by Timoshenko [1]. Articles published by Rendulic [4], Chwalla [5] and Miles [6] considered single panels stiffened along the two sides. All three authors used a closed form solution. They had, however, the analysis of webs of steel girders in

mind and not plates stiffened by interior ribs. This is also obvious in the article by Stiffel [17], where the plate is subjected to in-plane bending and the stresses were assumed to vary linearly across the plate width. Therefore, the distribution of the stiffeners was adjusted to the stress distribution.

Timoshenko [1] derived an open form solution to the problem of side simply supported plates stiffened by interior ribs, using again the minimum potential energy theorem. Because the assumed deflection surface must satisfy the boundary conditions, a double Fourier series was used to describe the buckled plate surface. According to their location in the system, the ribs are subjected to varying amounts of bending. Equating to zero the strain energy of the bent plate and ribs and the work done during buckling by the compressive forces acting on the plate and the ribs along the ends, an equation for the critical stress is found. It consists of a quotient with several infinite series of sine functions, involving the unknown number of half-waves i in the longitudinal direction, and the equally unknown number k of half waves in the transverse direction. Equating to zero the partial derivatives of this expression with respect to the unknown coefficients, an infinite system of homogeneous simultaneous equations was obtained. By equating to zero the determinant of this system of equations, an equation to determine the critical stress resulted. However, only buckling modes that are symmetrical with respect to the middle axis can be obtained by this method, if there is an even number of ribs. Three more important assumptions had to be made before any practical calculations could be considered:

1. The system buckles into one longitudinal half-wave;
that is, $i = 1$.
2. A very small number of equations, and thus coefficients,
is sufficiently accurate to determine the critical stress.
3. There are only very few ribs (one or two).

In this open form solution approach, the numerical problems for systems with several ribs and for the inclusion of a large number of equations (or coefficients) increased at such a rate as to render this method impractical. Even for the case of one rib only, assumptions 1 and 2 were very restrictive. Another disadvantage is the limitation to the side simply supported plate. A bridge type system with flexible side supports could not be handled, since the basic deflection surface could no longer be described by a double Fourier series alone.

Lokshin [14] developed a closed form solution for the buckling of a rectangular, longitudinally stiffened plate that was simply supported on all four sides. The ribs were assumed to be uniform and equidistant and subject only to bending about their transverse axis in addition to axial compression. Recurrence equations for the rib-line deflections and moments in the transverse direction made the form of the buckling determinant independent of the number of ribs. With the assumption of a single half wave sine variation of these rib-line deformations and moments, a simple buckling criterion evolved.

Barbré [7] in his dissertation also used a closed form solution approach to the problem. The governing differential equation and the corresponding Levy solution for the single panel with arbitrary side boundary conditions was found, plus four conditions of continuity at the

rib lines between each two panels. These conditions were equal deflections, equal transverse slope, moment equilibrium and shear force equilibrium. Thus the ribs were assumed to be subjected to transverse loads and to torsion. With a total of four boundary conditions for the plate and the four conditions of continuity for each rib, eight simultaneous equations were obtained for a plate with one interior rib, twelve equations for two interior ribs, etc.

Equating to zero the determinant of coefficients, solutions were found for plates with one rib at an arbitrary interior location and with simply supported or fixed sides. Both symmetric and anti-symmetric modes of buckling were investigated. For the case of two ribs, the system of equations became unbearably large and complicated for arbitrary boundary conditions and rib locations. Only a side simply supported plate with two equal and symmetrically arranged ribs was investigated, since with these simplifying assumptions the terms in the determinant of coefficients reduced considerably.

One of the goals of Barbré's paper was to find that critical ratio of the flexural rigidities of the ribs to the bending stiffness of the plate that causes local buckling. For any ratio larger than the critical one, only local buckling will occur and only system buckling for smaller ratios.

Based partially on the findings of Barbré, Bleich [8] presented side simply supported plates with one arbitrarily located rib or with two equal and equidistant ribs. The torsional rigidity of these ribs was neglected. Diagrams were presented that show the limiting value of the ratio of rib-to-plate stiffness as a function of the plate dimensions,

the cross sectional area of one rib and the number of half-waves in the longitudinal direction. Whereas in all the above mentioned references, completely elastic behavior of the material was assumed, Bleich included inelastic behavior in the derivation of the governing differential equation and in its solutions.

Another approach was taken by Wittrick [9]. There the system of panels and ribs was treated separately for each element. Since it can be assumed that the buckled surface of each element always has a sine variation in the longitudinal direction, so do also the rib lines. Therefore, the lateral deflections, rotations, forces and moments along a rib line will also vary sinusoidally and with the same wave length as the element deflections. Based on this distribution of the panel edge displacements and stresses, for each element an in-plane (or membrane) and an out-of-plane (or flexural) stiffness matrix was formulated. These matrices related the amplitudes of the edge forces and moments to the corresponding edge deflections and rotations. With the known stiffness matrices, equations of equilibrium at the line junctions of the elements were formulated. This led to a series of homogeneous simultaneous equations relating the displacements and rotations of all the line junctions to each other. At instability the determinant of coefficients of these equations is equal to zero and this constitutes the buckling criterion. The solution to this stability determinant is carried out exactly in the same manner as for the plate without stiffeners described on page 7. As Wittrick pointed out, there will be, in general, four equations of equilibrium at each rib line. This leads to a very large number of simultaneous equations and to very large stability determinants. The

computational problem becomes immense for an increasing number of panels and ribs.

In the field of civil engineering, the development of the orthotropic bridge deck made it necessary to find workable solutions for plates reinforced by longitudinal and transverse stiffeners. Orthotropic plate analysis [10,15,16] is based on the replacement of the ribbed plate by an equivalent continuum obtained by smearing out the rib properties. The result is a continuum model whose element stiffness is non-isotropic. Continuous field solutions are found, but the step of replacing the discrete continuous system by a continuum lacks a rational basis.

The finite element analysis [11] is another open form approach. The amount of work involved depends directly on the number of ribs and the size of the plate. There is, of course, great freedom with respect to the arbitrary spacing of the ribs or their dimensions and properties as well as in satisfying different boundary conditions. However, for every single problem the element properties, dimensions, etc. have to be restated. This method lends itself to the solution of special cases which are not tractable by other methods.

2.3. Closed Form Field or Functional Approach to Ribbed Plates

It has been shown that an important step in the buckling analysis of ribbed plates lies in the derivation of a closed form solution that will give a stability criterion, or a stability determinant, which is independent of the number of ribs. A closed form solution for the deformations and forces of a ribbed plate under lateral loads, which is independent of the number of ribs, has been found by Dean [12]. His functional solution yields deflections and forces at any desired point throughout

the plate simply by substituting the coordinates into the solution formula, which is valid at all points. As in [8], the first important step is to find the membrane and flexural stiffness matrices for the individual elements, that is, for the panels and the ribs. Since Dean was concerned with deformations and forces, the stiffness matrices do not include the effects of compressive stresses applied at the ends.

Of the two independent variables of the plate that describe the overall system, one is discrete and the other continuous. The continuous variable designates distance along a rib line and the discrete variable designates the rib under consideration. For simply supported plates, the solution is written as a double Fourier series containing an infinite number of terms with respect to the continuous variable and a finite number of terms with respect to the discrete variable. For flexible side supports, corrective terms are added to the double series. By the assumption of an infinite Fourier series representation with respect to the continuous variable, the continuous and the discrete variable are uncoupled. The attention is then turned to the determination of functions representing the variation with respect to the discrete variable.

2.4. Summary of Literature

In the buckling analysis of ribbed plates in compression, there are available exact, closed form solutions for plates having simple or fixed side supports and one interior rib with arbitrary location and torsional rigidity. For plates with two ribs exact closed form solutions exist only for simple support conditions and for equal and symmetrically arranged ribs. For each separate case, the number of ribs and the boundary conditions lead to separate systems of equations and to separate

buckling determinants.

Wittrick [9] also provides an exact solution. Again, for each number of ribs a different determinant of coefficients is set up. Theoretically, both Wittrick and Barbré [7] allow for arbitrary side boundary conditions and set no limits on the number of ribs, on the properties of the individual ribs and on their locations and spacing. Wittrick's solution also is the only one that allows for stiffeners that behave as deep beams (flat strips) and not only as one-dimensional beams as assumed in engineering theory. The above mentioned approaches all lead to large systems of complicated simultaneous equations that always depend on the number of ribs. For practical reasons, however, all these solutions are limited to very few ribs.

The approach taken by Timoshenko necessitates the additional and rather limiting assumptions of simple side supports, symmetrical buckling modes in the transverse direction and only one half-wave for the buckling in the longitudinal direction. The purely numerical approach of the finite element analysis is rather free with respect to the number of ribs, their locations and dimensions. However, each individual problem has to be set up completely from the beginning. There is also the question of accuracy and convergence of the solution, which may make necessary a variation of the kind or number of elements used. Approximations of a different kind are obtained by the orthotropic plate analysis where the rib properties are smeared out. The results show gross behavior at best and fail to have a rational basis.

3. Purpose of Investigation

None of the existing solutions to the ribbed plate in compression allows for a simple and exact approach, which is independent of the number of ribs and which incorporates arbitrary boundary conditions, deep beam type stiffeners and symmetric and anti-symmetric buckling modes. In this paper, therefore, a closed form approach is taken in which a functional solution is found that yields the buckling load for any number of panels and stiffeners. At the same time a solution is provided for the deflections and rotations of the rib lines under a combination of in-plane compressive and out-of-plane transverse loads as long as the compressive stresses remain well below the buckling level. The solution for the deformations of the rib lines can easily be extended to any point in the plate and will reflect local behavior.

The main goal of this thesis is the determination of the initial buckling of a ribbed plate using the adjacent equilibrium (or bifurcation) criterion. Postbuckling behavior is not investigated. The general approach is divided into two major parts, a Non-Composite Flexural Analysis for systems having negligible in-plane deformations and a Composite Membrane Analysis for systems having negligible flexural resistance. In each part, a distinction is made between plates having simple end and simple side supports and plates having simple end and flexible side supports. The torsional rigidity of interior and boundary ribs always is taken into account and the distinction is made between local and system buckling.

From the buckling criteria, it is possible to determine the boundary case between system and local buckling and thus to determine the

critical ratio of rib-to-plate stiffness which helps in the design of the stiffeners. For the simple buckling criterion, all the parameters can be inserted directly. These parameters are the panel and rib properties, the dimensions, and the number of ribs. The number of half-waves in the longitudinal and transverse direction has to be assumed. For each combination of half-wave values there will be one smallest eigenvalue that satisfies the buckling criterion. The correct buckling mode is the one that yields the absolute smallest eigenvalue. Because of the iteration procedure, this solution, as well as all the other solutions mentioned in the literature, makes necessary the use of high speed digital computer and renders impractical (or impossible) any solution by hand.

Since this investigation is primarily concerned with a field approach for a bridge type system and a solution that is independent of the number of ribs, the assumption of uniform and equidistant interior ribs has been made. However, the two boundary ribs can be chosen arbitrarily to reflect any kind of boundary condition from free sides to simple side supports and from zero torsional rigidity to fixed supports. Ribs and plate may be constructed of different materials. As in the literature, other assumptions are a constant modulus of elasticity, constant Poisson's ratio, linear stress strain relations, purely elastic behavior, perfectly flat plate, isotropic material, no residual stresses and uniformly applied compressive stresses along the two simply supported ends of the plate.

CHAPTER II

NON-COMPOSITE FLEXURAL ANALYSIS

In this section, the flexural analysis of a ribbed plate structure under uniformly applied stress at the ends is presented. The structure is proportioned so that the effects of the in-plane plate deformations and the T-beam action can be ignored in determining the stiffness matrices of the elements that comprise the structure. This results in a simpler and lower order model than would otherwise be the case. It is assumed that the system acts as a flexural plate supported by rib-beams that are not longitudinally constrained at the rib plate junction. The junction is detailed such that the torsional stiffness of the rib is taken into account.

1. Derivation of Boundary Force-Deformation Relations

A typical panel between two ribs is shown in Fig. 7.

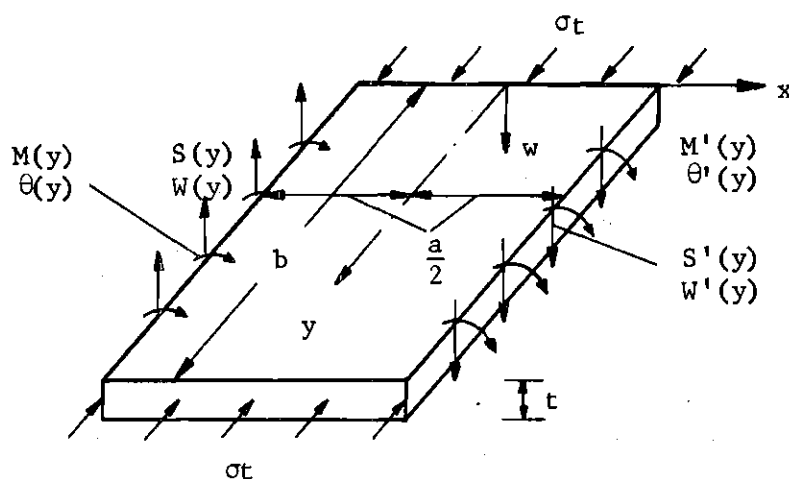


Figure 7. Panel with Boundary Forces and Deformations for the Non-Composite Flexural Analysis.

1.1. Governing Differential Equation

The first step of this analysis is to determine the set of coefficients relating the out-of-plane edge forces M and S and the in-plane compressive force N_y to the edge deformations θ and W for the elements that comprise the system. The fourth order partial differential equation for the thin flat plate subject to a uniform longitudinal stress resultant N_y is given by

$$D_x^4 w + 2D_x^2 D_y^2 w + (D_y^2 + \frac{1}{D} N_y) D_y^2 w = 0 \quad (1)$$

where D_x and D_y denote the differential operators $\frac{\partial}{\partial x}$ and $\frac{\partial}{\partial y}$.

The plate is simply supported out-of-plane at the extremities of the y -coordinate, that is, the following boundary equations apply:

$$w(x, 0) = M_y(x, 0) = 0$$

These boundary conditions are natural to a Fourier series analysis and the Levy solution for general boundary conditions along the sides, or at $x = \pm \frac{a}{2}$ can be written as follows:

$$w(x, y) = \sum_{i=1}^{\infty} X_i(x) \cdot \sin \alpha_i y \quad \alpha_i = \frac{i\pi}{b} \quad (2)$$

Substitution of Eq. 2 into the governing differential Eq. 1 yields

$$\left\{ D_x^4 - 2\alpha_i^2 D_x^2 + \alpha_i^2 (\alpha_i^2 - \frac{1}{D} N_y) \right\} X_i(x) = 0$$

an ordinary differential equation of fourth order, having the general solution,

$$X_i(x) = A_i e^{m_1 x} + B_i e^{m_2 x} + C_i e^{m_3 x} + D_i e^{m_4 x} \quad (3)$$

and the following four roots

$$m_{1,2} = \pm \alpha_i \sqrt{1 + \frac{\eta}{\alpha_i}} \quad m_{3,4} = \pm \alpha_i \sqrt{1 - \frac{\eta}{\alpha_i}} \quad (4)$$

where $\eta^2 = \frac{N_y}{D}$.

From Eq. 4, it is seen that there are only real roots for $\eta < \alpha_i$, or $N_y < \frac{i^2 \pi^2 D}{b^2}$, which yields, after rewriting Eq. 3,

$$X_i(x) = A_i \sinh m_1 x + B_i \cosh m_2 x + C_i \sinh m_3 x + D_i \cosh m_4 x \quad (5)$$

For $\eta = \alpha_i$, or $N_y = \frac{i^2 \pi^2 D}{b^2}$, there are two pairs of real double roots,

$$m_{1,2} = \pm \sqrt{2} \cdot \alpha_i \quad m_{3,4} = 0 \quad (6)$$

and Eq. 3 becomes

$$X_i(x) = A_i \sinh \sqrt{2} \alpha_i + B_i \cosh \sqrt{2} \alpha_i + C_i + D_i x$$

The most important case for this investigation is given by $\eta > \alpha_i$,

or $N_y > \frac{i^2 \pi^2 D}{b^2}$, from which a pair of real and a pair of imaginary roots is obtained:

$$m_{1,2} = \pm \alpha_i \sqrt{\frac{\eta}{\alpha_i} + 1} \quad m_{3,4} = \pm \sqrt{-1} \alpha_i \sqrt{\frac{\eta}{\alpha_i} - 1} \quad (7)$$

and the following expression for $X_i(x)$,

$$X_i(x) = A_i \sinh m_1 x + B_i \cosh m_1 x + C_i \sin m_3 x + D_i \cos m_3 x$$

For zero-in-plane loads, that is, for $N_y = 0$ or $\eta = 0$, Eq. 4 yields two identical pairs of real roots,

$$m_{1,2,3,4} = \pm \alpha_i \quad (8)$$

and

$$X_i(x) = A_i \sinh \alpha_i x + B_i \cosh \alpha_i x + C_i \alpha_i x \sinh \alpha_i x + D_i \alpha_i x \cosh \alpha_i x$$

which is the same result as in Reference [12].

The interest here is in obtaining relations between boundary forces and displacements, which are related to the displacement function $w(x,y)$. These forces and moments along the panel edges and the panel edge deformations also vary sinusoidally and with the same half-wave length b/i . They can be expressed as infinite series with respect to the y -coordinate as follows:

$$\begin{bmatrix} \tilde{D}_x w(-\frac{a}{2}, y) \\ \frac{1}{a} w(-\frac{a}{2}, y) \\ \tilde{D}_x w(\frac{a}{2}, y) \\ \frac{1}{a} w(\frac{a}{2}, y) \end{bmatrix} = \begin{bmatrix} \theta(y) \\ W(y) \\ \theta'(y) \\ W'(y) \end{bmatrix} = \sum_{i=1}^{\infty} \begin{bmatrix} \theta \\ W \\ \theta' \\ W' \end{bmatrix}_i \sin \alpha_i y \quad (9)$$

$$\begin{bmatrix} m_x(-\frac{a}{2}, y) \\ Q_x(-\frac{a}{2}, y) + \tilde{D}_y m_{xy}(-\frac{a}{2}, y) \\ -m_x(\frac{a}{2}, y) \\ Q_x(\frac{a}{2}, y) + \tilde{D}_y m_{xy}(\frac{a}{2}, y) \end{bmatrix} = \begin{bmatrix} M(y) \\ S(y) \\ M'(y) \\ S'(y) \end{bmatrix} = \sum_{i=1}^{\infty} \begin{bmatrix} M \\ S \\ M' \\ S' \end{bmatrix}_i \sin \alpha_i y \quad (10)$$

where, according to Reference [1],

$$\begin{aligned}
m_{xy} &= D(1 - \nu) \tilde{D}_x \tilde{D}_y w \\
m_x &= -D(\tilde{D}_x^2 + \nu \tilde{D}_y^2) w \\
Q_x &= -D \tilde{D}_x (\tilde{D}_x^2 + \tilde{D}_y^2) w \\
S &= -D \tilde{D}_x [\tilde{D}_x^2 + (2 - \nu) \tilde{D}_y^2] w
\end{aligned}$$

1.2. Flexural Stiffness Matrix

Depending on the parameter η , four cases must be considered in order to obtain the solution for the plate with general boundary conditions on the two sides. In each case, the resulting force-deformation relations can be expressed in the following form,

$$\begin{bmatrix} M \\ aS \\ M' \\ aS' \end{bmatrix}_i = \frac{D}{a} \begin{bmatrix} d_{11} & d_{12} & d_{13} & -d_{14} \\ -d_{12} & -a^2 \alpha^2 d_{22} & -d_{14} & a^2 \alpha^2 d_{24} \\ d_{13} & d_{14} & d_{11} & -d_{12} \\ -d_{14} & -a^2 \alpha^2 d_{24} & -d_{12} & a^2 \alpha^2 d_{22} \end{bmatrix}_i \begin{bmatrix} \theta \\ W \\ \theta' \\ W' \end{bmatrix}_i \quad (11)$$

The value of these coefficients will now be determined for each case.

Case 1: $N_y < \frac{i^2 \pi^2 D}{b^2}$

The general solution is given by Eqs. 2, 4, and 5. Eq. 9 furnishes the four boundary conditions from which the four constants of integration can be determined. This leads to the following four equations, presented in matrix notation:

$$\begin{bmatrix}
 \frac{\xi}{a} \cosh \frac{\xi}{2} & -\frac{\xi}{a} \sinh \frac{\xi}{2} & \frac{\zeta}{a} \cosh \frac{\zeta}{2} & -\frac{\zeta}{a} \sinh \frac{\zeta}{2} \\
 -\sinh \frac{\xi}{2} & \cosh \frac{\xi}{2} & -\sinh \frac{\zeta}{2} & \cosh \frac{\zeta}{2} \\
 \frac{\xi}{a} \cosh \frac{\xi}{2} & \frac{\xi}{a} \sinh \frac{\xi}{2} & \frac{\zeta}{a} \cosh \frac{\zeta}{2} & \frac{\zeta}{a} \sinh \frac{\zeta}{2} \\
 \sinh \frac{\xi}{2} & \cosh \frac{\xi}{2} & \sinh \frac{\zeta}{2} & \cosh \frac{\zeta}{2}
 \end{bmatrix}_i \begin{Bmatrix} A \\ B \\ C \\ D \end{Bmatrix}_i = \begin{Bmatrix} \theta \\ W \\ \theta' \\ W' \end{Bmatrix}_i$$

where $\xi = m_1 a$ and $\zeta = m_3 a$

and m_1 and m_3 are defined by Eq. 4.

Solving these equations for A_i , B_i , C_i , and D_i yields

$$\begin{bmatrix} A \\ C \end{bmatrix}_i = I_i \begin{bmatrix} \sinh \frac{\zeta}{2} & -\frac{\zeta}{a} \cosh \frac{\zeta}{2} \\ -\sinh \frac{\xi}{2} & \frac{\xi}{a} \cosh \frac{\xi}{2} \end{bmatrix}_i \begin{Bmatrix} \theta' + \theta \\ W' - W \end{Bmatrix}_i$$

$$\begin{bmatrix} B \\ D \end{bmatrix}_i = I'_i \begin{bmatrix} \cosh \frac{\zeta}{2} & -\frac{\zeta}{a} \sinh \frac{\zeta}{2} \\ -\cosh \frac{\xi}{2} & \frac{\xi}{a} \sinh \frac{\xi}{2} \end{bmatrix}_i \begin{Bmatrix} \theta' - \theta \\ W' + W \end{Bmatrix}_i$$

where $1/I_i = 2 \left(\frac{\xi}{a} \sinh \frac{\zeta}{2} \cosh \frac{\xi}{2} - \frac{\zeta}{a} \sinh \frac{\xi}{2} \cosh \frac{\zeta}{2} \right)$

and $1/I'_i = 2 \left(\frac{\xi}{a} \sinh \frac{\xi}{2} \cosh \frac{\zeta}{2} - \frac{\zeta}{a} \sinh \frac{\zeta}{2} \cosh \frac{\xi}{2} \right)$

This solution will now be used to express the Euler coefficients of the plate edge forces from Eq. 10 in terms of the coefficients of the edge deformations, Eq. 9. This results in the previously stated Eq. 11 and the individual terms of that equation in this case are as follows:

$$d_{11} = \frac{1}{J_i} (\xi^2 - \zeta^2) (\xi \sinh \zeta \cosh \xi - \zeta \sinh \xi \cosh \zeta)$$

$$d_{12} = \frac{1}{J_i} \left\{ \xi \zeta (\xi^2 + \zeta^2) (1 - \nu) (\cosh \xi \cosh \zeta - 1) - \left[2\xi^2 \zeta^2 - \frac{\nu}{2} (\xi^2 + \zeta^2)^2 \right] \sinh \xi \sinh \zeta \right\}$$

$$d_{13} = \frac{1}{J_i} (\xi^2 - \zeta^2) (\zeta \sinh \xi - \xi \sinh \zeta)$$

$$d_{14} = \frac{1}{J_i} (\xi^2 - \zeta^2) \xi \zeta (\cosh \xi - \cosh \zeta)$$

$$a^2 \alpha_i^2 d_{22} = \frac{1}{J_i} (\xi^2 - \zeta^2) \xi \zeta (\xi \sinh \xi \cosh \zeta - \zeta \sinh \zeta \cosh \xi)$$

$$a^2 \alpha_i^2 d_{24} = \frac{1}{J_i} (\xi^2 - \zeta^2) \xi \zeta (\xi \sinh \xi - \zeta \sinh \zeta)$$

$$J_i = \frac{a^2}{I_i I_i'} = (\xi^2 + \zeta^2) \sinh \xi \sinh \zeta + 2\xi \zeta (1 - \cosh \xi \cosh \zeta)$$

$$\text{Case 2: } N_y = \frac{i^2 \pi^2 D}{b^2}$$

Proceeding as in case 1, the four equations from which the constants of integration can be determined are found to be the following:

$$\begin{bmatrix} \frac{\xi}{a} \cosh \frac{\xi}{2} & -\frac{\xi}{a} \sinh \frac{\xi}{2} & 0 & 1 \\ -\sinh \frac{\xi}{2} & \cosh \frac{\xi}{2} & 1 & -\frac{a}{2} \\ \frac{\xi}{a} \cosh \frac{\xi}{2} & \frac{\xi}{a} \sinh \frac{\xi}{2} & 0 & 1 \\ \sinh \frac{\xi}{2} & \cosh \frac{\xi}{2} & 1 & \frac{a}{2} \end{bmatrix}_i \begin{bmatrix} A \\ B \\ C \\ D \end{bmatrix}_i = \begin{bmatrix} \theta \\ W \\ \theta' \\ W' \end{bmatrix}_i$$

where $\xi = m_1 \cdot a$ and m_1 is defined by Eq. 6.

Solving for A_i through D_i yields

$$\begin{Bmatrix} A \\ D \end{Bmatrix}_i = I_i \cdot \begin{bmatrix} \frac{a}{2} & -1 \\ -\sinh \frac{\xi}{2} & \frac{1}{a} \cosh \frac{\xi}{2} \end{bmatrix}_i \begin{Bmatrix} \theta' + \theta \\ W' - W \end{Bmatrix}_i$$

$$\begin{Bmatrix} B \\ C \end{Bmatrix}_i = I_i' \cdot \begin{bmatrix} 1 & 0 \\ -\cosh \frac{\xi}{2} & \frac{1}{a} \sinh \frac{\xi}{2} \end{bmatrix}_i \begin{Bmatrix} \theta' - \theta \\ W' + W \end{Bmatrix}_i$$

where $1/I_i = 2(\frac{\xi}{2} \cosh \frac{\xi}{2} - \sinh \frac{\xi}{2})$

and $1/I_i' = \frac{2\xi}{a} \cdot \sinh \frac{\xi}{2}$

The individual terms of Eq. 11 in this case are given below:

$$d_{11} = \frac{1}{J_i} \xi^2 (\xi \cosh \xi - \sinh \xi)$$

$$d_{12} = \frac{1}{J_i} \xi^3 [(1 - \nu)(\cosh \xi - 1) + 1/2 \nu \xi \sinh \xi]$$

$$d_{13} = \frac{1}{J_i} \xi^2 (\sinh \xi - \xi)$$

$$d_{14} = \frac{1}{J_i} \xi^3 (\cosh \xi - 1)$$

$$a^2 \alpha_i^2 d_{22} = a^2 \alpha_i^2 d_{24} = \frac{1}{J_i} \xi^4 \sinh \xi$$

$$J_i = \frac{a}{I_i I_i'} = \xi^2 \sinh \xi + 2\xi(1 - \cosh \xi)$$

$$\text{Case 3: } N_y > \frac{i^2 \pi^2 D}{b^2}$$

It is seen later that this is the most important case. All buckling loads found for simple side supports for flexible side supports are obtained using the formulas belonging to case 3. The equations to determine the constants of integration are the following:

$$\begin{bmatrix} \frac{\xi}{a} \cosh \frac{\xi}{2} & -\frac{\xi}{a} \sinh \frac{\xi}{2} & \frac{\zeta}{a} \cos \frac{\zeta}{2} & \frac{\zeta}{a} \sin \frac{\zeta}{2} \\ -\sinh \frac{\xi}{2} & \cosh \frac{\xi}{2} & -\sin \frac{\zeta}{2} & \cos \frac{\zeta}{2} \\ \frac{\xi}{a} \cosh \frac{\xi}{2} & \frac{\xi}{a} \sinh \frac{\xi}{2} & \frac{\zeta}{a} \cos \frac{\zeta}{2} & -\frac{\zeta}{a} \sin \frac{\zeta}{2} \\ \sinh \frac{\xi}{2} & \cosh \frac{\xi}{2} & \sin \frac{\zeta}{2} & \cos \frac{\zeta}{2} \end{bmatrix}_i \begin{Bmatrix} A \\ B \\ C \\ D \end{Bmatrix}_i = \begin{Bmatrix} \theta \\ W \\ \theta' \\ W' \end{Bmatrix}_i$$

where $\xi = m_1 a$ $\zeta = m_3 a$,

m_1 and m_3 are defined by Eq. 7

and the constants of integration are found to be

$$\begin{Bmatrix} A \\ B \end{Bmatrix}_i = I_i \cdot \begin{bmatrix} \sin \frac{\zeta}{2} & -\frac{\zeta}{a} \cos \frac{\zeta}{2} \\ -\sinh \frac{\xi}{2} & \frac{\xi}{a} \cosh \frac{\xi}{2} \end{bmatrix}_i \begin{Bmatrix} \theta' - \theta \\ W' - W \end{Bmatrix}_i$$

$$\begin{Bmatrix} C \\ D \end{Bmatrix}_i = I_i' \cdot \begin{bmatrix} \cos \frac{\zeta}{2} & \frac{\zeta}{a} \sin \frac{\zeta}{2} \\ -\cosh \frac{\xi}{2} & \frac{\xi}{a} \sinh \frac{\xi}{2} \end{bmatrix}_i \begin{Bmatrix} \theta' - \theta \\ W' - W \end{Bmatrix}_i$$

where $1/I_i = 2 \left(\frac{\xi}{a} \sin \frac{\zeta}{2} \cosh \frac{\xi}{2} - \frac{\zeta}{2} \sinh \frac{\xi}{2} \cos \frac{\zeta}{2} \right)$

and $1/I_i' = 2 \left(\frac{\xi}{a} \sinh \frac{\xi}{2} \cos \frac{\zeta}{2} + \frac{\zeta}{a} \sin \frac{\zeta}{2} \cosh \frac{\xi}{2} \right)$.

The individual terms of Eq. 11 for case 3 are listed below:

$$d_{11} = \frac{1}{J_i} (\xi^2 - \zeta^2) (\xi \cosh \xi \sin \zeta - \zeta \sinh \xi \cos \zeta)$$

$$d_{12} = \frac{1}{J_i} \left\{ (1 - \nu) \xi \zeta (\xi^2 - \zeta^2) (\cosh \xi \cos \zeta - 1) \right. \\ \left. + \left[2\xi^2 \zeta^2 + \frac{\nu}{2} (\xi^2 - \zeta^2)^2 \right] \cdot \sinh \xi \sin \zeta \right\}$$

$$d_{13} = \frac{1}{J_i} (\xi^2 + \zeta^2) (\zeta \sinh \xi - \xi \sin \zeta)$$

$$d_{14} = \frac{1}{J_i} (\xi^2 + \zeta^2) \xi \zeta (\cosh \xi - \cos \zeta)$$

$$a^2 \alpha_i^2 d_{22} = \frac{1}{J_i} (\xi^2 + \zeta^2) \xi \zeta (\xi \sinh \xi \cos \zeta + \zeta \cosh \xi \sin \zeta)$$

$$a^2 \alpha_i^2 d_{24} = \frac{1}{J_i} (\xi_2 + \zeta^2) \xi \zeta (\xi \sinh \xi + \zeta \sin \zeta)$$

$$J_i = \frac{a^2}{I_i I_i} = (\xi^2 - \zeta^2) \sinh \xi \sin \zeta + 2\xi \zeta (1 - \cosh \xi \cos \zeta)$$

Case 4: $N_y = 0$

This plate corresponds to the plate under transverse loads only. The out-of-plane stiffness that will be found can only be used to determine the displacements of such a plate. The individual terms of Eq. 11 for this case are the following:

$$d_{11}, d_{22} = \frac{1}{J_i} \xi (\sinh 2\xi + 2\xi)$$

$$d_{13}, d_{24} = \frac{1}{J_i} 2\xi (\xi \cosh \xi + \sinh \xi)$$

$$d_{12} = \frac{1}{J_i} \xi^2 \{ (1 - \nu) \xi^2 + (1 - \nu) \sinh^2 \xi \}$$

$$d_{14} = \frac{1}{J_i} 2\xi^3 \sinh \xi$$

$$J_i = \sinh^2 \xi - \xi^2$$

$\xi = m_1 a$, where m_1 is defined by Eq. 8.

This completes the derivation of the boundary force-deformation equations, or the stiffness matrices, for the Non-Composite Flexural Analysis.

The stiffeners can be considered as plates having one free edge. Corresponding simplified stiffness matrices can easily be derived by

setting $M_1' = S_1' = 0$ in Eq. 11. In that case, θ_1' and W_1' also can be eliminated from the same equation. An alternate procedure is to treat the ribs using elementary beam theory. The governing differential equations for beams under out-of-plane and in-plane forces in addition to axial compression are derived in the Appendix.

2. Derivation of the Buckling Criteria

2.1. Equilibrium Equations

The two equations of equilibrium for a rib line element (Fig. 8) for the Non-Composite Flexural Analysis are

$$\begin{aligned} M(r,y) + M'(r-1,y) + \bar{M}(r,y) &= M^e(r,y) \\ S(r,y) - S'(r-1,y) - \bar{N}(r,y) &= -P^e(r,y) \end{aligned} \quad (12)$$

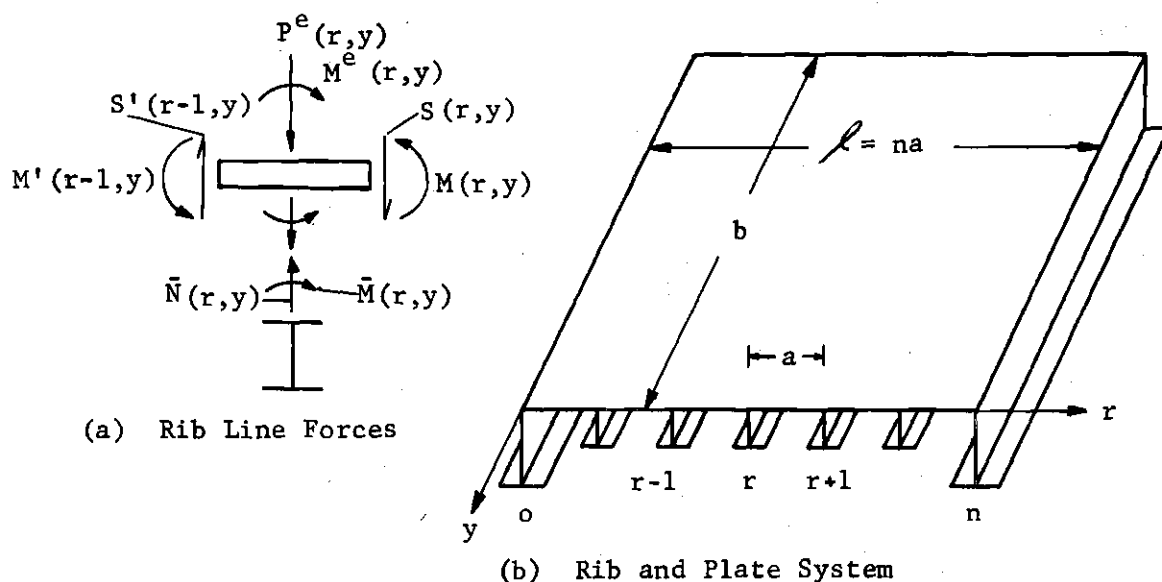


Figure 8. Non-Composite Flexural Model

Here $M(r,y)$, $M'(r,y)$, $S(r,y)$, $S'(r,y)$ are the plate boundary moments and shear resultants on the typical panel r between the rib lines r and $r + 1$. They are defined below in a manner analogous to Eq. 10, where they were shown without the discrete variable r , designating the appropriate rib and panel.

$$\begin{bmatrix} M(r,y) \\ S(r,y) \\ M'(r,y) \\ S'(r,y) \end{bmatrix} = \sum_{i=1}^{\infty} \begin{bmatrix} M(r) \\ S(r) \\ M'(r) \\ S'(r) \end{bmatrix}_i \cdot \sin \alpha_i y \quad \alpha_i = \frac{i\pi}{b} \quad (13)$$

$\bar{M}(r,y)$ and $\bar{N}(r,y)$ are the distributed twisting moments and direct forces transmitted to the rib. Details and physical properties frequently encountered are such that $\bar{M}(r,y)$ can be considered negligible. On the other hand, retention of this term does not greatly complicate the mathematical model. It will be retained for a more general solution and can be dropped in those cases in which it is not applicable.

$M^e(r,y)$ and $P^e(r,y)$ are the equivalent applied line moments and loads which are comprised of the actual rib line quantities M^a and P^a , if any, and the fixed edge panel quantities M^f , M'^f , S^f , and S'^f due to mid panel loads $q(x,y)$ (Figure 9), that is:

$$M^e(r,y) = M^a(r,y) - M^f(r,y) - M'^f(r-1,y)$$

$$P^e(r,y) = P^a(r,y) - S^f(r,y) - S'^f(r-1,y)$$

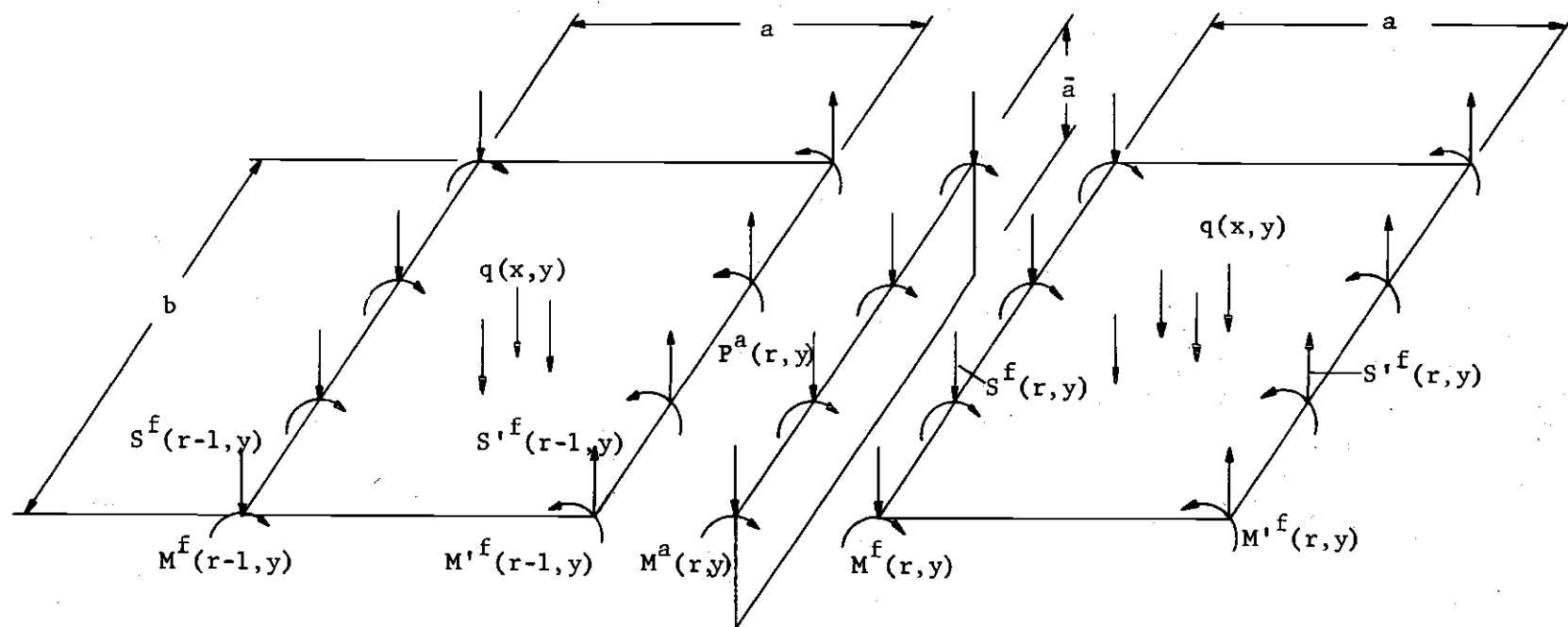


Figure 9. Applied Rib Line and Fixed Edge Panel Forces and Moments

The distributed twisting moments and direct forces transmitted to the ribs and the equivalent line loads can also be expressed in series form, that is,

$$\begin{pmatrix} \bar{M}(r,y) \\ \bar{N}(r,y) \\ P^e(r,y) \\ M^e(r,y) \end{pmatrix} = \sum_{i=1}^{\infty} \begin{pmatrix} \bar{M}_i(r) \\ \bar{N}_i(r) \\ P_i(r) \\ M_i^e(r) \end{pmatrix} \sin \alpha_i y \quad (14)$$

Replacement of all quantities in Eqs. 12 by their equivalent series and matching like coefficients results in the following relations between the series coefficients:

$$M_i(r) + M_i'(r-1) + \bar{M}_i(r) = M_i^e(r) \quad (15)$$

$$S_i(r) - S_i'(r-1) + \bar{N}_i(r) = -P_i(r)$$

2.2. Displacements

The panel force coefficients M_i , M_i' , S_i , and S_i' in these equations can be expressed in terms of the coefficients of the rib line deflections and rotations, Eqs. 9, by use of the plate stiffness coefficients shown in Eq. 11. The stiffness coefficients used for the ribs, \bar{M}_i and \bar{N}_i , are those derived by beam theory in the Appendix, Eqs. 76 and 87.

Note that U_i for the beam in Eq. 87 must be replaced by W_i for use in Eq. 15 for the rib line, or panel edge, deflection. The necessary relationships are thus:

$$\begin{aligned}
M_i(r) &= \frac{D}{a} [d_{11}\theta_i(r) + d_{12}W_i(r) + d_{13}\theta_i'(r) - d_{14}W_i'(r)] \\
M_i'(r-1) &= \frac{D}{a} [d_{13}\theta_i(r-1) + d_{14}W_i(r-1) + d_{11}\theta_i'(r-1) - \\
&\quad - d_{12}W_i'(r-1)] \\
\bar{M}_i(r) &= \frac{D}{a} \left[\frac{a}{D} \alpha_i^2 k_B \theta_i(r) \right] \\
S_i(r) &= \frac{D}{a} \left[-\frac{1}{a} d_{12}\theta_i(r) - a\alpha_i^2 d_{22}W_i(r) - \frac{1}{a} d_{14}\theta_i'(r) + \right. \\
&\quad \left. + a\alpha_i^2 d_{24}W_i'(r) \right] \\
S_i'(r-1) &= \frac{D}{a} \left[-\frac{1}{a} d_{14}\theta_i(r-1) - a\alpha_i^2 d_{24}W_i(r-1) - \frac{1}{a} d_{12}\theta_i'(r-1) + \right. \\
&\quad \left. + a\alpha_i^2 d_{22}W_i'(r-1) \right] \\
\bar{N}_i(r) &= \frac{D}{a} \left[\frac{a^2 \alpha_i^2}{D} (P - \alpha_i^2 B) W_i(r) \right]
\end{aligned} \tag{16}$$

Note also the following expressions of continuity at the rib lines:

$$\begin{aligned}
\theta'(r-1) &= \theta(r) \\
W'(r-1) &= W(r) \\
\theta'(r) &= \theta(r+1) \\
W'(r) &= W(r+1)
\end{aligned} \tag{17}$$

2.3. Governing Difference Equations for the Rib Line Deformations

Introducing Debla, ∇ , the second central difference operator, and Multa, \square , the mean difference operator, that is

$$\begin{aligned}
\nabla_r F(r) &= F(r+1) - 2F(r) + F(r-1) \\
\square_r F(r) &= 1/2 [F(r+1) - F(r-1)]
\end{aligned} \tag{18}$$

and substituting the force deformation relations, Eqs. 24, into the equilibrium relations, Eqs. 22 and 23, yields

$$\begin{bmatrix} d_{13}(\Delta_r + 2\gamma_i') & -2d_{14}\Delta_r \\ -2d_{14}\Delta_r & a^2\alpha_i^2 d_{24}(\Delta_r - 2\bar{\gamma}_i') \end{bmatrix} \begin{bmatrix} \theta_i(r) \\ w_i(r) \end{bmatrix} = \frac{a}{D} \begin{bmatrix} M_i^e(r) \\ -aP_i(r) \end{bmatrix} \quad (19)$$

in which

$$\gamma_i' = 1 + \frac{d_{11}}{d_{13}} + \frac{a}{2Dd_{13}} \alpha_i^2 \bar{k}B'$$

$$\bar{\gamma}_i' = -1 + \frac{d_{22}}{d_{24}} + \frac{a}{2Dd_{24}} (\alpha_i^2 B - P)$$

where $\bar{k}B'$ is the torsional stiffness of the rib beams, and

B is the flexural rigidity of the rib beams about the axis parallel to the plate.

Eq. 19 constitutes the uncoupled difference equations for the plate that is simply supported at the ends and stiffened longitudinally with equal and equally spaced ribs. This equation can be used to obtain rib line displacements for low axial loads or to derive the buckling criterion for initial buckling for the Non-Composite Flexural Model.

3. Simple Side Supports

The physical boundary conditions for the case of simple side supports are zero deflections and zero external moments at $r = 0$ and n or

$$\begin{aligned} w_i(0) &= w_i(n) = 0 \\ M_i(0) + \bar{M}_i(n) - M_i^e(0) &= 0 \end{aligned} \quad (20)$$

$$M_i'(n-1) + \bar{M}_i(n) - M_i^e(n) = 0$$

Selecting a boundary beam torsional stiffness equal to one half of the stiffness of the interior beams, that is, $(\bar{k}B')^b = 1/2\bar{k}B'$, Eq. 76 from the Appendix becomes, at $r = 0$,

$$\bar{M}_i(0) = + \frac{1}{2} \alpha_i^2 \bar{k}B' \theta_i(0)$$

Substitution of this equation and Eq. 11 into the second Eq. 20 and recalling Eqs. 17 yields the boundary conditions on the left and right hand sides of the plate

$$d_{13} [\Delta_r + \gamma_i'] \theta_i(0) - d_{14} [\Delta_r + 1 - \frac{d_{12}}{d_{14}}] w_i(0) = 0 \quad (21)$$

$$d_{13} [\gamma_i' - \nabla_r] \theta_i(n) + d_{14} [1 - \frac{d_{12}}{d_{14}} - \nabla_r] w_i(n) = 0$$

where γ_i' is defined by Eq. 19 and

$\Delta_r F(r) = F(r+1) - F(r)$ is the first forward,

$\nabla_r F(r) = F(r) - F(r-1)$ is the first backward difference operator.

The most convenient form of solution for the case of simple side supports is that of a double series, that is, the Euler coefficients in Eq. 19 are expressed as finite series as follows:

$$\begin{aligned}
 \begin{bmatrix} \theta_i(r) \\ \frac{1}{\varphi_r} M_i^e(r) \end{bmatrix} &= \sum_{k=0}^n \begin{bmatrix} \theta_{ik} \\ M_{ik}^\varphi \end{bmatrix} \cdot \cos \frac{k\pi r}{n} \\
 \begin{bmatrix} W_i(r) \\ P_i(r) \end{bmatrix} &= \sum_{k=1}^{n-1} \begin{bmatrix} W_{ik} \\ P_{ik} \end{bmatrix} \cdot \sin \frac{k\pi r}{n}
 \end{aligned} \tag{22}$$

where

$$\varphi_r = \begin{cases} 1 & \text{for } r = 1, (1), n-1 \\ 1/2 & \text{for } r = 0, n \end{cases}$$

Not that the complete expression, for example for $\theta(r,y)$ is a finite-infinite double series as follows:

$$\theta(r,y) = \sum_{i=1}^{\infty} \sum_{k=0}^n \theta_{ik} \cos \frac{k\pi r}{n} \sin \alpha_i y$$

Attention is called to the device of expanding a weighted moment coefficient function instead of the function itself. This allows one to satisfy the inhomogeneous moment boundary conditions. Eqs. 20, without adding corrective boundary functions, which are needed for functions expressed as finite sine series. The weighted moment function coefficient is found from the following equation

$$M_{ik}^\varphi = \frac{2\varphi_k}{n} \sum_{r=0}^n M_i^e(r) \cos \frac{k\pi r}{n}$$

When substituting Eqs. 22 into Eq. 19, the operators Debla, ∇ , and Multa, \square , will operate onto the trigonometric terms and this yields

$$\begin{aligned}
\Delta_r \theta_i(r) &= -2 \sum_{k=0}^n \theta_{ik} \alpha_k \cos \frac{k\pi r}{n} \\
\Delta_r W_i(r) &= -2 \sum_{k=1}^{n-1} W_{ik} \alpha_k \sin \frac{k\pi r}{n} \\
\bar{\Delta}_r \theta_i(r) &= - \sum_{k=0}^n \theta_{ik} \sin \frac{k\pi}{n} \sin \frac{k\pi r}{n} \\
\bar{\Delta}_r W_i(r) &= + \sum_{k=1}^{n-1} W_{ik} \sin \frac{k\pi}{n} \cos \frac{k\pi r}{n}
\end{aligned} \tag{23}$$

where $\alpha_k = 1 - \cos \frac{k\pi}{n}$.

With these terms, Eq. 19 becomes, after matching like coefficients,

$$2 \begin{bmatrix} d_{13}(\gamma_i' - \alpha_k) & -d_{14} \sin \frac{k\pi}{n} \\ d_{14} \sin \frac{k\pi}{n} & -a^2 d_i^2 d_{24}(\bar{\gamma}_i' + \alpha_k) \end{bmatrix} \begin{bmatrix} \theta_{ik} \\ W_{ik} \end{bmatrix} = \frac{a}{D} \begin{bmatrix} M_{ik}^\varphi \\ -aP_{ik} \end{bmatrix} \tag{24}$$

Solving this equation for θ_{ik} and W_{ik} yields

$$\begin{Bmatrix} \theta_{ik} \\ W_{ik} \end{Bmatrix} = \frac{a}{2D |C_{ik}'|} \begin{bmatrix} a^2 \alpha_i^2 d_{24}(\bar{\gamma}_i' + \alpha_k) & d_{14} \sin \frac{k\pi}{n} \\ d_{14} \sin \frac{k\pi}{n} & d_{13}(\gamma_i' - \alpha_k) \end{bmatrix} \begin{Bmatrix} M_{ik}^\varphi \\ aP_{ik} \end{Bmatrix} \tag{25}$$

where $C_{ik}' = -a^2 \alpha_i^2 d_{13} d_{24}(\gamma_i' - \alpha_k)(\bar{\gamma}_i' + \alpha_k) + d_{14}^2 \alpha_k(2 - \alpha_k)$

Note that $\sin^2 \frac{k\pi}{n} = \alpha_k(2 - \alpha_k)$

This completes the solution for the deformations of the rib lines under axial compressive and lateral loads applied to the whole structure.

4. Buckling with Simple Side Supports

Eq. 25 has non-trivial solutions for zero external loads and moments, that is for $M_{ik} = P_{ik} = 0$, only when C_{ik}' , the determinant of coefficients, vanishes. C_{ik}' is a function of i and k and the compressive loads P and N_y . For each set of i and k there exists an infinite number of load combinations for which $C_{ik}' = 0$. These load combinations in general can be found only by using a trial and error method. The smallest of all the possible load combinations for all possible sets of i and k constitutes the initial buckling load.

In the course of this procedure, it was found that buckling loads N_{cr} , plus a corresponding P , are always defined by "case 3" of the solutions to the partial differential equation for the panel element, that is, for $N_y > \alpha_i^2 D$.

The expression for $C_{ik}' = 0$ can be solved explicitly for P which yields

$$P_{cr} = \frac{i^2 \pi^2 B}{b^2} + \frac{2D}{a} \left[d_{22} - d_{24}(1 - \alpha_k) - \frac{d_{14}^2 \cdot \alpha_k \cdot (2 - \alpha_k)}{a^2 \alpha_i^2 d_{13}(\gamma_i' - \alpha_k)} \right]$$

The second term of this expression approaches zero as t , and therefore, D approaches zero; that is, for the extreme case of a structure that consists only of ribs. The first term is the Euler buckling load of a column which is simply supported at both ends. Therefore, it is seen that the solution to the problem of the stiffened plate is limited on one side by the simple column buckling case.

On the other hand, C_{ik}' cannot be solved explicitly for N_y . However, setting A and P equal to zero and then solving $C_{ik}' = 0$ by a trial and error method yields a smallest value for N_y equal to the buckling

load of a flat, unstiffened plate which is simply supported on all four sides, that is

$$N_{cr} = \frac{\pi^2 D}{\ell^2} \left(\frac{b}{i\ell} + \frac{i\ell}{b} \right)^2$$

where $\ell = n \cdot a$ is the total width of the plate and $k = 1$.

This is the other extreme of the stiffened plate problem. The same result can be obtained directly from Eqs. 11 and Case 3 by setting $a = \ell$, $W_i = W_i' = 0$, and $\theta_i = -\theta_i'$. This results in

$$\theta_i = \frac{\ell}{D} \cdot \frac{1}{d_{11} - d_{13}} \cdot M_i$$

which increases above all bounds for $d_{11} = d_{13}$ or

$$\xi \sin \zeta (\cosh \xi + 1) - \zeta \sinh \xi (\cos \zeta + 1) = 0$$

This equation is satisfied for $n = \pi$ which yields

$$\pi = \ell \cdot \frac{i\pi}{b} \sqrt{\frac{\eta}{\alpha_1} - 1}$$

or

$$N_{cr} = \frac{\pi^2 D}{\ell^2} \left(\frac{b}{i\ell} + \frac{i\ell}{b} \right)^2$$

Up to this point the compressive force per unit length, N_y , acting on the panels between the ribs, and the axial load, P , acting on the ribs have been kept distinct. This allowed for an additional degree of freedom in the buckling analysis. However, for most practical cases, the plate will be constructed in such a way that N_y and P cause uniform strains in panels and ribs. When panels and ribs have the same modulus of elasticity,

this corresponds to a uniform stress, σ . Therefore, N_y and P can be expressed as follows

$$N_y = \sigma t \quad P = \sigma A$$

where t is the panel thickness and A is the cross sectional area of one rib.

In the case of a concrete plate stiffened by steel ribs, the stress σ in the plate would be replaced by $f = \sigma \frac{\bar{E}}{E}$ where \bar{E} is the modulus of elasticity of the concrete.

A group of special eigenvalues of C_{ik} is obtained by setting k equal to n , that is by prescribing as many half-waves in the transverse direction of the buckled surface as there are panels. Then the rib lines correspond to the node lines of the buckling surface. By assumption, the rib lines remain straight, that is they do not buckle. This is called local buckling. From this mode, buckling stresses equal to those of flat plates of width " a " must be expected. The trial and error method does indeed furnish this expected result. In other words, for k equal to n the stress at buckling of the plate of width ℓ , length b , thickness t and flexural rigidity D , with n panels of equal width a between $n + 1$ stiffeners of equal flexural properties is found to be

$$\sigma_{cr} = \frac{1}{t} \frac{\pi^2 D}{a^2} \left(\frac{b}{ia} + \frac{ia}{b} \right)^2$$

or, since $a = \ell/n$

$$\sigma_{cr} = \frac{1}{t} \frac{\pi^2 D}{\ell^2} \cdot k_{cr} \quad (26)$$

where $k_{cr} = n^2 \left(\frac{b}{ia} + \frac{ia}{b} \right)^2$.

The maximum values of k for values of $n = 1, 2, 3, \dots$ are

$$k = 4, 16, 36, \dots$$

In general the initial buckling may occur in any number of half-waves $1 \leq k \leq n$ in the transverse direction. The two most important parameters, besides ℓ , b and n , are the two ratios

$$\gamma = \frac{B}{\ell D} \quad \delta = \frac{A}{\ell t}$$

where B and A are the flexural rigidity and cross sectional area of one rib.

There are now possible two major approaches to make use of the buckling criteria $C_{ik}' = 0$. One is to find that value of γ for given values of ℓ , b , n and δ which causes local buckling to occur at smaller stresses than system buckling. This approach is important in the design of structures when system buckling, at least initially, is to be avoided. The sought value of γ corresponds to a minimum rib stiffness B , in comparison to the plate rigidity D , that guarantees local buckling to occur first.

It should be noted that the ratio δ , is multiplied through with σ , represents the ratio P/N_y for a plate made from materials having the same modulus of elasticity for panels and stiffeners.

The other approach is to find the critical stress σ_{cr} for a fully chosen set of parameters. This corresponds to finding k_{cr} in Eq. 26.

In the process of obtaining numerical results, it is seen that $k = 1$, that is the first symmetric mode, yields the lowest k_{cr} , except for the case of local buckling. With $k = 1$ and introducing the definitions of σ_{cr} , γ_i' , and $\bar{\gamma}_i'$ into the expression for C_{ik}' from Eq. (25) yields the following simplified buckling criterion

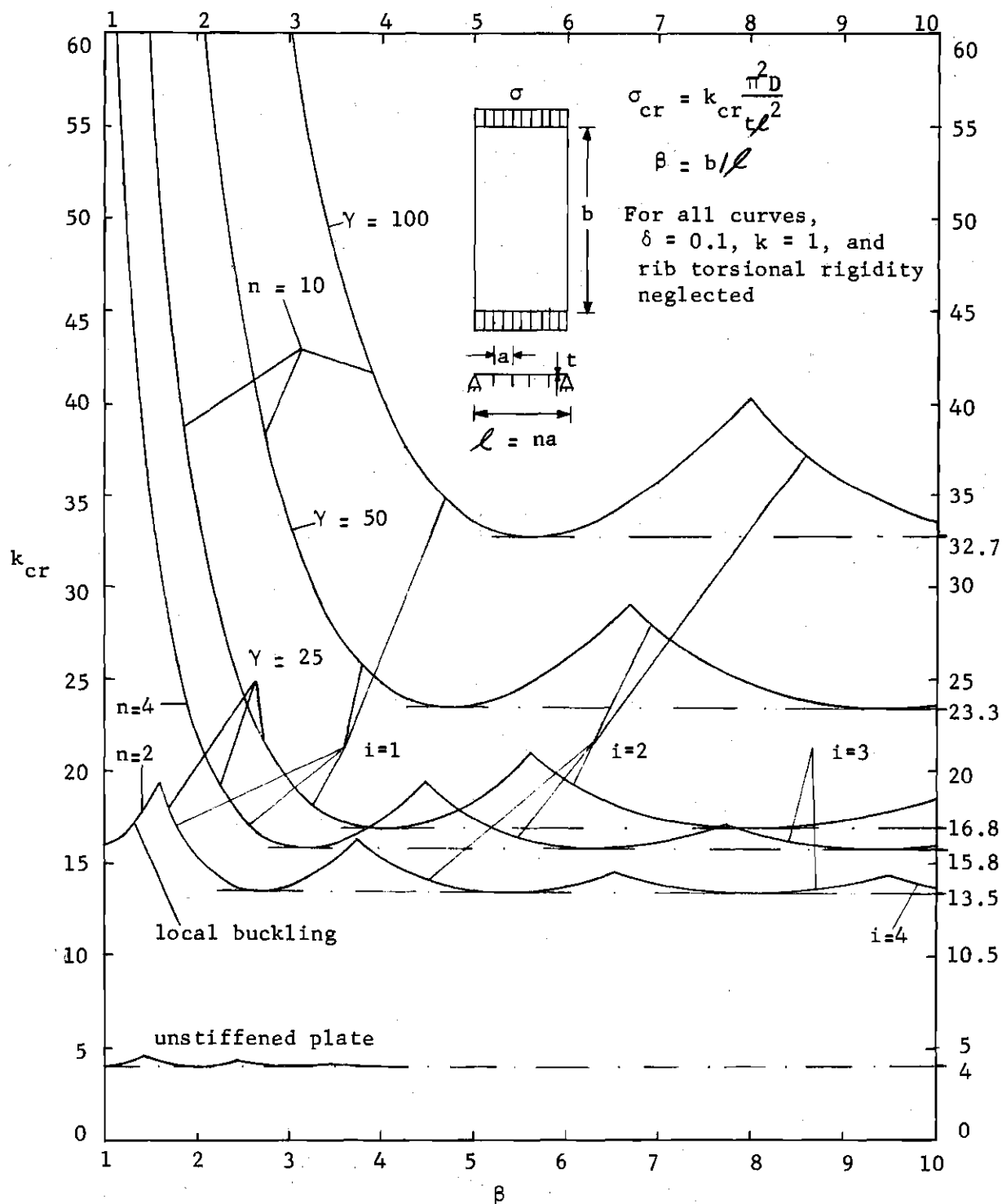
$$\frac{\pi^2 i^2}{4\beta^2} d_{11} \left[d_{22} + \frac{\pi^2}{2n} \left(\frac{n^2 i^2}{\beta^2} \gamma - k_{cr} \delta \right) \right] - d_{14}^2 = 0$$

where $\beta = b/\ell$ is the plate aspect ratio and the torsional rigidity of the ribs has been neglected.

The buckling criterion in this latest form reveals that k_{cr} depends only on n , γ , δ and the ratio i/β since the stiffness coefficients d also are functions of k_{cr} , n , and i/β . Larger values for k_{cr} can be expected for high ratios of γ/δ rather than low ones. Prescribing a set of values for i , β , n , γ , and δ , the corresponding value for k_{cr} can be found by iteration. Only the curve for $i = 1$ needs to be determined, however, since the curves for $i = 2, 3$, etc. can be obtained by doubling, tripling, etc. of the abscissas of the points on the curve for $i = 1$.

4.1. Numerical Examples for Simple Side Supports

In Figure 10 some curves are shown for k_{cr} as a function of β , n , and γ . Comparison to the curve for an unstiffened plate shows the similarity of the basic form of these relations. In both, stiffened and unstiffened plates, a lowest value of k_{cr} is approached asymptotically with increasing β . The transition point from buckling into one, two, three, etc. longitudinal half-waves shifts to larger aspect ratios with an increase in the number of ribs and in their stiffnesses. The relative


 Plate 10. Curves for k_{cr} for Simple Side Supports

gain in the buckling strength is greatest for the first rib and decreases for additional ribs. For $\beta > 1$, substantial increases in the rib stiffnesses are necessary to bring the buckling strength of the ribbed plate anywhere near the strength in the local buckling mode.

The curve for $n = 2$ checks well with data given by Timoshenko in [1]. All values are slightly lower, however, and thus represent an improved and decreased upper bound for the initial buckling. The curve for $n = 4$ in turn checks with data given in the USS Steel Design Manual [18] as far as the graphs presented there permit accurate numerical interpretation. The curves for $n = 10$, or for any number of n greater than 4, represent new data unavailable in this form up to now.

5. Boundary Deflections

The second solution of the Non-Composite Flexural Analysis of a ribbed plate is for the unloaded system, that is for $M_i^e(r) = P_i(r) = 0$, with imposed boundary deflections which can be represented by a symmetric and anti-symmetric component, that is, by

$$W_i^s = \frac{1}{2} [W_i(0) + W_i(n)]$$

$$W_i^{a/s} = \frac{1}{2} [W_i(0) - W_i(n)]$$

A technique to include the imposed boundary deflections in the Fourier series assumptions is to add corrective terms to the classic series. For the symmetric component, or $W_i^{a/s} = 0$, the solution can be written in the following form:

$$\bar{\theta}_i^s(r) = W_i^s \sum_{k=1,3,\dots}^n \bar{\theta}_{ik} \cos \frac{k\pi r}{n} \quad (27)$$

$$\bar{w}_i^s(r) = W_i^s \left(\sum_{k=1,3,\dots}^{n-1} \bar{w}_{ik} \sin \frac{k\pi r}{n} + 1 \right)$$

Substitution of Eq. 27 into the governing differential equation (Eq. 19) and into the boundary conditions (Eq. 21) and matching like coefficients shows that only odd terms of k are used, which justifies the assumptions of Eq. 27. Solving for $\bar{\theta}_{ik}$ and \bar{w}_{ik} yields

$$\bar{\theta}_{ik} = - \frac{2a^2 \alpha_i^2 d_{24} \varphi_k}{n |C_{ik}'|} \left\{ d_{14} \bar{\gamma}_i' (2 - \sigma_k) + (d_{12} - d_{14}) (\bar{\gamma}_i' + \sigma_k) \right\}$$

$$\bar{w}_{ik} = - \frac{2(2 - \sigma_k)}{n \sin \frac{k\pi}{r} |C_{ik}'|} \left\{ d_{14} (d_{12} - d_{14}) \sigma_k + a^2 \alpha_i^2 d_{13} d_{24} \bar{\gamma}_i' (\gamma_i' - \sigma_k) \right\}$$

For the anti-symmetric component, or $W_i^s = 0$, the solution can be written in the following form

$$\bar{\theta}_i^{a/s}(r) = W_i^{a/s} \sum_{k=2,4,\dots}^{n-1} \bar{\theta}_{ik} \cos \frac{k\pi r}{n} \quad (28)$$

$$\bar{w}_i^{a/s}(r) = W_i^{a/s} \left\{ \sum_{k=2,4,\dots}^{n-1} \bar{w}_{ik} \sin \frac{k\pi r}{n} + \left(1 - \frac{2r}{n}\right) \right\}$$

where $\bar{\theta}_{ik}$ and \bar{w}_{ik} are identical to the ones for the symmetric case. Note the term $(1 - 2r/n)$ which increases from zero at $r = n/2$ to ± 1 at the boundaries and which reflects anti-symmetry.

6. Rib Boundaries

The total solution for a Non-Composite Flexural Analysis of a ribbed plate is that for a plate with flexible ribs for side supports (Fig. 10).

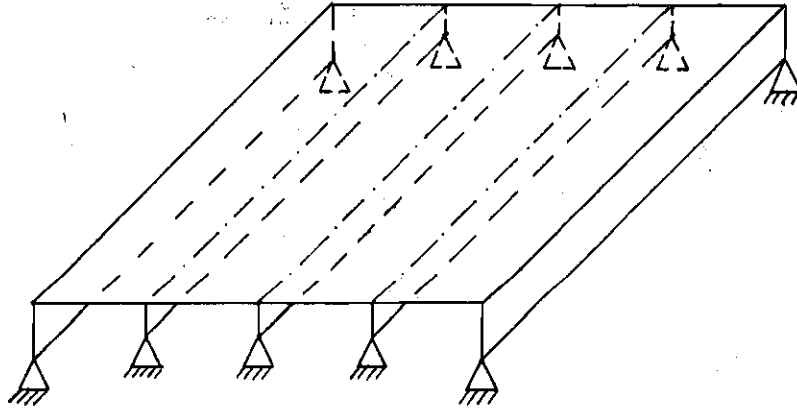


Figure 11. Plate with Rib Boundaries

It can be obtained by superposition of Eqs. 22, 27, and 28 and is written as follows:

$$\theta_i^t(r) = \theta_i(r) + \bar{\theta}_i^s(r) + \bar{\theta}_i^{a/s}(r)$$

$$W_i^t(r) = W_i(r) + \bar{W}_i^s(r) + \bar{W}_i^{a/s}(r)$$

That combination of the solutions for simple side supports and boundary deflection cases has to be found which satisfies the rib boundary conditions at $r = 0, n$. The coefficients of the boundary deflections, W_i^s and $W_i^{a/s}$, must be determined through study of the conditions at the boundary beams. The two boundary ribs are assumed to be identical so that the structure is symmetric about $r = n/2$. The interior ribs may or may not be identical to the boundary ribs. One can determine W_i^s and $W_i^{a/s}$ by

working with the symmetric and anti-symmetric components separately, that is for k odd and for k even, respectively. The coefficients of the symmetric and the anti-symmetric components of the boundary loadings are written in a similar way as the boundary deflections, that is

$$P_i^s = 1/2 [P_i(0) + P_i(n)] \quad P_i^{a/s} = 1/2 [P_i(0) - P_i(n)] \quad (29)$$

For the symmetric component of the solution, consider the equilibrium along the rib line $r = 0$, that is the second of Eqs. 15 becomes:

$$S_i(0) + \bar{N}_i(0) + P_i^s(0) = 0 \quad (30)$$

where $S_i(r)$ and $\bar{N}_i(r)$ are defined by Eqs. 16.

Substitution of these terms into Eq. 30 yields the boundary condition in terms of the boundary rib displacements

$$-d_{14}(\Delta_r + \epsilon_i^{'b})\theta_i^t(0) + a^2\alpha_i^2d_{24}(\Delta_r - \bar{\gamma}_i^{'b})w_i^t(0) + \frac{a^2}{D}P_i^s = 0$$

$$\text{where } \epsilon_i^{'b} = \frac{d_{14} + d_{12}}{d_{14}}$$

$$\bar{\gamma}_i^{'b} = \bar{\epsilon}_i^{'b} + \frac{a}{Dd_{24}}(\alpha_i^2B^b - P)$$

$$\bar{\epsilon}_i^{'b} = \frac{d_{22} - d_{24}}{d_{24}}$$

B^b is the boundary beam flexural rigidity and

Δ_r is defined as in Eq. 21.

Substitution of $\theta_i^t(r)$ and $W_i^t(r)$ into the boundary condition and solving for W_i^s yields

$$W_i^s = \frac{\frac{a^2}{D} P_i^s + s_i^s(0)}{\eta_i^{,b} - \bar{s}_i^s(0)}$$

where

$$\eta_i^{,b} = \frac{a^4 \alpha_i^2 (\alpha_i^2 B^b - P)}{aD} \quad \eta_i^{,b} = \frac{a^4 \alpha_i^2 (\alpha_i^2 B^b - P)}{aD}$$

$$s_i^s(0) = -d_{14} \sum_{k=1,3,\dots}^n (\epsilon_i^{,b} - \sigma_k) \theta_{ik} + a^2 \alpha_i^2 d_{24} \sum_{k=1,3,\dots}^{n-1} W_{ik} \sin \frac{k\pi}{n}$$

$$\bar{s}_i^s(0) = -d_{14} \sum_{k=1,3,\dots}^n (\epsilon_i^{,b} - \sigma_k) \bar{\theta}_{ik} + a^2 \alpha_i^2 d_{24} \left(\sum_{k=1,3,\dots}^{n+1} \bar{W}_{ik} \sin \frac{k\pi}{n} - \bar{\epsilon}_i^{,b} \right)$$

The last two terms are the coefficients of the panel boundary shears of the two parts of the total solution.

The anti-symmetric component of the boundary deflection is obtained in a similar way as the symmetric component and is found to be

$$W_i^{a/s} = \frac{\frac{a^2}{D} P_i^{a/s} + s_i^{a/s}(0)}{\eta_i^{,b} - \bar{s}_i^{a/s}(0)}$$

where $\eta_i^{,b}$ is defined as in the symmetric case

and

$$s_i^{a/s}(0) = -d_{14} \sum_{k=0,2,\dots}^n (\epsilon_i^{,b} - \sigma_k) \theta_{ik} + a^2 \alpha_i^2 d_{24} \left(\sum_{k=2,4,\dots}^{n-1} W_{ik} \sin \frac{k\pi}{n} \right)$$

$$\bar{s}_i^{a/s}(0) = -d_{14} \sum_{k=0,2,\dots}^n (\epsilon_i^{,b} - \sigma_k) \bar{\theta}_{ik} + a^2 \alpha_i^2 d_{24} \left(\sum_{k=2,4,\dots}^{n-1} \bar{w}_{ik} \sin \frac{k\pi}{n} - \bar{\epsilon}_i^{,b} \right)$$

This completes the solution of the deflections of a ribbed plate with beam boundaries subject to lateral and in-plane compressive loads and using a Non-Composite Flexural Analysis.

7. Buckling with Rib Boundaries

For the plate with beam boundaries, the buckling criteria have taken a new form. Now, the buckling stresses can be found from the conditions that $\theta_i^t(r)$ or $W_i^t(r)$ increase above all bounds. This occurs, on the one hand, for $C_{ik}' = 0$, the same criterion as for the previous case of simple side supports. The term C_{ik}' appears as the denominator of the expressions for θ_{ik} , $\bar{\theta}_{ik}$, W_{ik} , and \bar{W}_{ik} . On the other hand, $\theta_i^t(r)$ and $W_i^t(r)$ also increase above all bounds for vanishing denominators of the expressions for W_i^s and $W_i^{a/s}$, that is, for one of the two following conditions:

$$\eta_i^{,b} - \bar{s}_i^s(0) = 0 \quad \text{and} \quad \frac{a^2}{D} P_i^s + s_i^s(0) \neq 0 \quad (31)$$

$$\eta_i^{,b} - \bar{s}_i^{a/s}(0) = 0 \quad \text{and} \quad \frac{a^2}{D} P_i^{a/s} + s_i^{a/s}(0) \neq 0$$

The new buckling criterion no longer depends on k . However, since local buckling still is determined by $C_{ik}' = 0$, it could be expected that Eq. 31 govern in cases of system buckling when its eigenvalues are lower than those found from $C_{ik}' = 0$. Both criteria have to be checked in order to determine which one of the two gives the lowest critical stress.

7.1. Numerical Examples for Rib Boundaries

For the symmetric case, Figure 12 shows some curves for k_{cr} as a function of β , n , γ , and the ratio B^b/B , that is the ratio of boundary rib bending stiffness to interior rib stiffness. Again, the torsional rigidity of the ribs has been neglected.

Comparison of the curves for simple side supports and rib boundaries shows great similarity, up to the point of the first minimum for simple side supports. As could be expected, this is especially true for very rigid boundary ribs. For aspect ratios near 1, local buckling controls. For ribbed plates with $B^b = B$, k_{cr} can well be approximated by Euler hyperbolas, that is these plates behave similarly to simple columns. Except for local buckling, $i = 1$ yields the lowest k_{cr} .

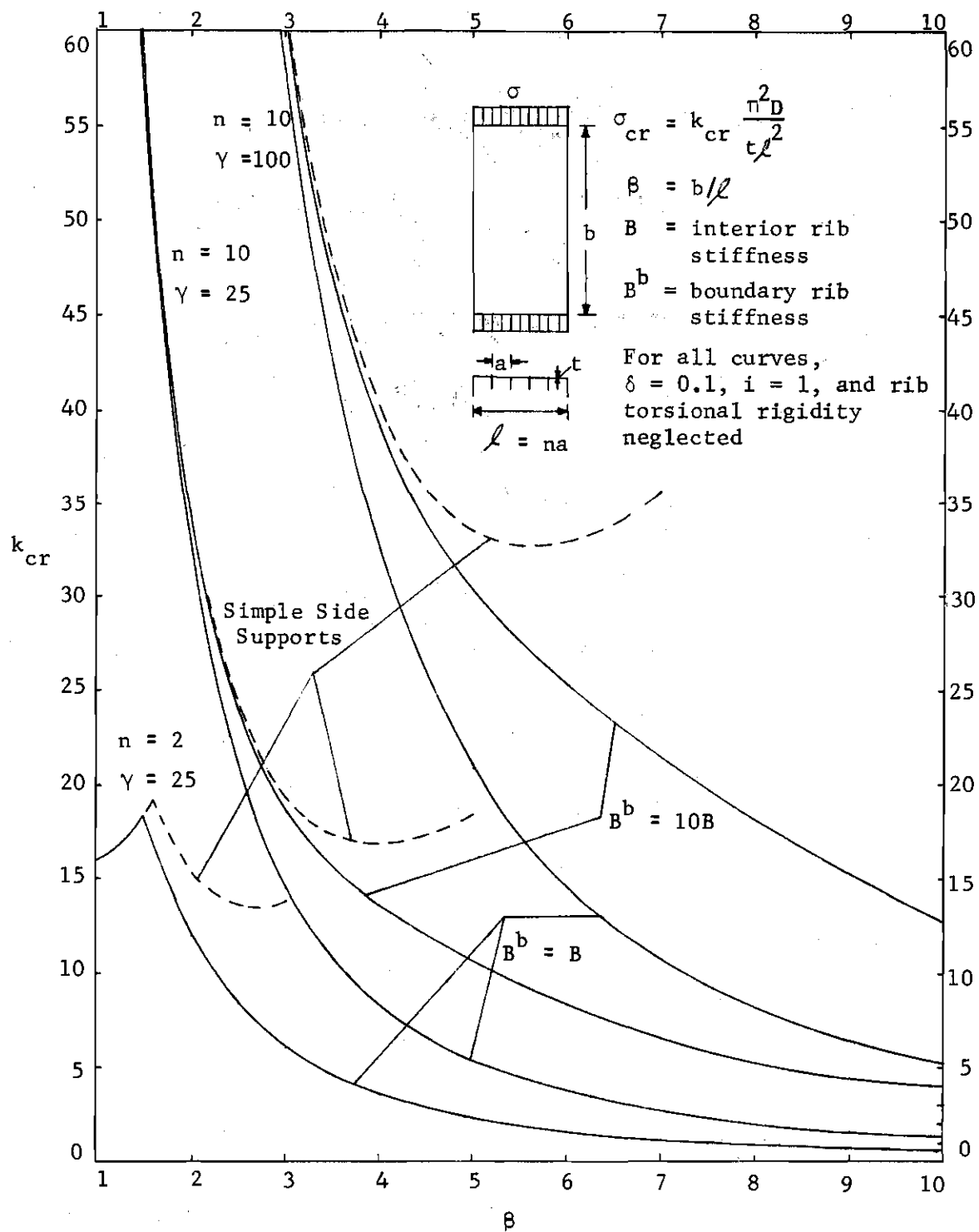


Figure 12. Curves for k_{cr} for Rib Boundaries,
Symmetric Boundary Deflections

CHAPTER III

COMPOSITE MEMBRANE ANALYSIS

In close analogy to the Non-Composite Flexural Analysis, the Composite Membrane Analysis of a ribbed plate structure under uniformly applied stresses at the ends is presented in this section. The structure is proportioned so that the effects of the out-of-plane deformations can be ignored in determining the stiffness matrices of the elements that comprise the structure. This again results in a simpler and lower order model as was the case in the previous chapter. One consequence of such an approximation is that the loads can theoretically be applied only along the rib lines. Thus, distributed loads must be replaced by their line load equivalents. Composite action--the T-beam effect--is taken into account by matching the longitudinal displacement at the top of the ribs to the y-component of the membrane displacements along the rib lines.

1. Derivation of Boundary Force-Deformation Relations

A typical panel between two ribs is shown in Figure 11.

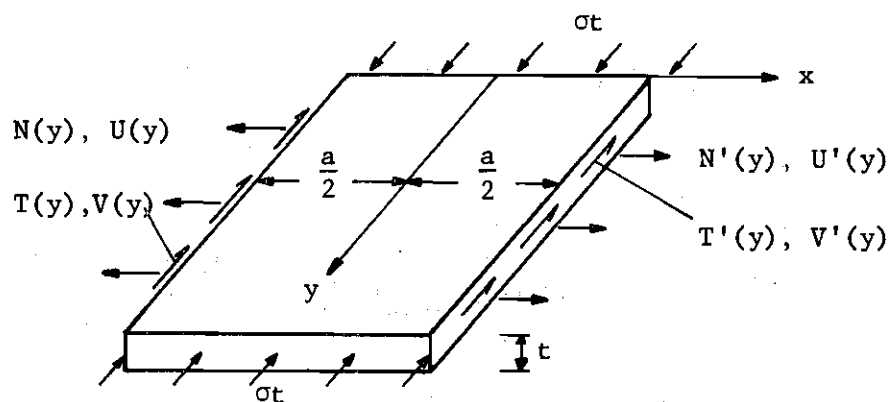


Figure 13. Panel with Boundary Forces and Deformations for the Composite Membrane Analysis

The first step of this analysis is the determination of the set of coefficients that relates the in-plane edge forces N , T , and σ to the edge deformations U and V for the elements of the structure. In anticipation of a similar result as in the Non-Composite Flexural Analysis, the general stiffness matrix equation for the Composite Membrane Analysis is written as follows:

$$\left\{ \begin{array}{c} N \\ T \\ N' \\ T' \end{array} \right\}_i = \left[\begin{array}{cccc} b_{11} & b_{12} & b_{13} & b_{14} \\ b_{12} & b_{22} & b_{14} & b_{24} \\ b_{13} & b_{14} & b_{11} & b_{12} \\ b_{14} & b_{24} & b_{12} & b_{22} \end{array} \right]_i \left\{ \begin{array}{c} U \\ V \\ U' \\ V' \end{array} \right\}_i \quad (32)$$

The elements of the stiffness matrix normally could be found by carrying out a routine plane stress analysis of the panel with zero body forces. This classical linear theory of elasticity is inadequate, however, to show the destabilizing effect of the longitudinal compressive stress, σ and a non-linear theory must be used instead. The derivations given here are based on those presented by Wittrick [9].

1.1 Governing Differential Equation

A non-linear theory which is suitable for this problem has been developed by Novozhilov [13]. The non-linearity, with which we are concerned, is that arising from the use of the deformed geometry of an element in formulating the equations of equilibrium. For the case of plane stress these may be written as follows (Eq. II, 48, Novozhilov):

$$\bar{D}_x \left[(1 + \bar{D}_x \bar{u}) \bar{n}_x + \bar{n}_{xy} \bar{D}_y \bar{u} \right] + \bar{D}_y \left[(1 + \bar{D}_x \bar{u}) \bar{n}_{yx} + \bar{n}_{xy} \bar{D}_y \bar{u} \right] = 0 \quad (33)$$

$$\bar{D}_y \left[(1 + \bar{D}_y \bar{v}) \bar{n}_y + \bar{n}_{yx} \bar{D}_x \bar{v} \right] + \bar{D}_x \left[(1 + \bar{D}_y \bar{v}) \bar{n}_{xy} + \bar{n}_{yx} \bar{D}_x \bar{v} \right] = 0$$

where \bar{n}_x , \bar{n}_y , \bar{n}_{xy} , and \bar{n}_{yx} are the stresses, and \bar{u} and \bar{v} are the displacements in the x and y directions from the unstrained state. In the basic state, the following relations correspond to the applied compressive stress:

$$\bar{n}_y = -\sigma, \bar{n}_x = \bar{n}_{xy} = 0, \bar{D}_y \bar{v} = -\frac{\sigma}{E}, \bar{D}_x \bar{u} = \nu \frac{\sigma}{E}, \bar{D}_y \bar{u} = \bar{D}_x \bar{v} = 0 \quad (34)$$

Eq. 33 is identically satisfied by Eqs. 34.

The additional stresses and displacements, after infinitesimally small in-plane edge forces have been applied, are n_x , n_y , n_{xy} , u , and v . In the final state, the relations in Eq. 34 are replaced by those shown below.

$$\begin{aligned} \bar{n}_y &= -\sigma + n_y & \bar{D}_y \bar{v} &= -\frac{\sigma}{E} + \bar{D}_y v \\ \bar{n}_x &= n_x & \bar{D}_x \bar{v} &= \bar{D}_x v \\ \bar{n}_{xy} &= n_{xy} & \bar{D}_y \bar{u} &= \bar{D}_y u \\ & & \bar{D}_x \bar{u} &= \nu \frac{\sigma}{E} + \bar{D}_x u \end{aligned}$$

Substitution of these expressions into Eq. 33 yields

$$\begin{aligned} -\sigma \bar{D}_y^2 v + (1 - \frac{\sigma}{E}) (\bar{D}_y n_y + \bar{D}_x n_{xy}) + \left[\bar{D}_y (n_{xy} \bar{D}_x v + n_{yx} \bar{D}_y v) \right. \\ \left. + \bar{D}_x (n_{xy} \bar{D}_y v + n_{yx} \bar{D}_x v) \right] = 0 \end{aligned} \quad (35)$$

$$- \sigma \tilde{D}_y^2 u + (1 + \frac{\nu \sigma}{E}) (\tilde{D}_x n_x + \tilde{D}_y n_{xy}) + \left[\tilde{D}_x (n_{xy} \tilde{D}_y u + n_x \tilde{D}_x u) + \tilde{D}_x (n_{xy} \tilde{D}_x u + n_y \tilde{D}_y u) \right] = 0$$

Since the additional stresses n_x , n_y , and n_{xy} are infinitesimal, and therefore the displacements u and v resulting from them also, the terms in square brackets in Eqs. 35 are small of second order with respect to the remaining terms and thus may be neglected. The terms σ/E and $\nu\sigma/E$ also are small compared to unity and will be neglected. Eq. 35 then simplifies to the following expressions:

$$\tilde{D}_y n_y + \tilde{D}_x n_{xy} - \sigma \tilde{D}_y^2 v = 0 \quad (36)$$

$$\tilde{D}_x n_x + \tilde{D}_y n_{xy} - \sigma \tilde{D}_y^2 u = 0$$

The stress strain relations for the additional stresses and displacements are identical with those of the linear elastic theory and are as follows:

$$n_y = \frac{E}{1 - \nu^2} (\tilde{D}_y v + \nu \tilde{D}_x u) \quad (37)$$

$$n_x = \frac{E}{1 - \nu^2} (\tilde{D}_x u + \nu \tilde{D}_y v)$$

$$n_{xy} = n_{yx} = \frac{E}{2(1 + \nu)} (\tilde{D}_y u + \tilde{D}_x v)$$

Substitution of Eqs. 37 into Eqs. 36 results in the following two simultaneous partial differential equations in u and v :

$$\begin{bmatrix} 2D_x^2 + (1 - \nu)\Phi^2 D_y^2 & (1 + \nu)D_x D_y \\ (1 + \nu)D_x D_y & (1 - \nu)D_x^2 + 2\varphi^2 D_y^2 \end{bmatrix} \begin{Bmatrix} u(x, y) \\ v(x, y) \end{Bmatrix} = \begin{Bmatrix} 0 \\ 0 \end{Bmatrix} \quad (38)$$

where $\varphi^2 = 1 - (1 - \nu^2) \cdot \epsilon$

$$\Phi^2 = 1 - 2(1 + \nu) \cdot \epsilon$$

and $\epsilon = \sigma/E$ is the uniform longitudinal compressive strain in the undeformed state. Note that neglecting ϵ with respect to unity in Eq. 38 would reduce it to the classic linear one and would mean the entire loss of the destabilizing effect of the compressive stress, σ .

Here the concern is with panels that are simply supported in the plane at the extremities of the y coordinate; that is, a partial statement of the boundary conditions is

$$n_y(x, 0) = n_y(x, b) = u(x, 0) = u(x, b) = 0 \quad (39)$$

Thus the solution, which is general with respect to the boundary conditions at $x = \pm a/2$, can be written as follows:

$$u(x, y) = \sum_{i=1}^{\infty} U_i(x) \sin \alpha_i y ; \quad v(x, y) = \sum_{i=1}^{\infty} V_i(x) \cos \alpha_i y \quad (40)$$

Substitution of Eq. 40 into Eq. 38 yields two ordinary simultaneous differential equations in $U_i(x)$ and $V_i(x)$

$$\begin{bmatrix} \alpha_i(1 + \nu)D_x & (1 - \nu)D_x^2 - 2\varphi^2\alpha_i^2 \\ 2D_x^2 - (1 - \nu)\Phi^2\alpha_i^2 & - (1 + \nu)\alpha_i D_x \end{bmatrix} \begin{Bmatrix} U_i(x) \\ V_i(x) \end{Bmatrix} = \begin{Bmatrix} 0 \\ 0 \end{Bmatrix}$$

which are transformed in the standard manner to a scalar stress function as follows:

$$U_i(x) = \left[(1 - \nu) D_x^2 - 2\varphi^2 \alpha_i^2 \right] F_i(x) \quad (41)$$

$$V_i(x) = -\alpha_i (1 + \nu) D_x F_i(x)$$

These equations identically satisfy the first differential equation, and the second equation becomes

$$\left\{ 2(1 - \nu) D_x^4 - \left[4\varphi^2 + (1 - \nu)^2 \Phi^2 - (1 + \nu)^2 \right] D_x^2 \alpha_i^2 + 2(1 - \nu) \Phi^2 \varphi^2 \alpha_i^4 \right\} F_i(x) = 0,$$

an ordinary differential equation of the fourth order with the general solution

$$F_i(x) = A_i e^{m_1 x} + B_i e^{m_2 x} + C_i e^{m_3 x} + D_i e^{m_4 x}$$

Substitution into Eq. 41 yields

(42)

$$U_i(x) = (-\varphi A_i \sinh \varphi \alpha_i x + B_i \sinh \Phi \alpha_i x) + (-\varphi C_i \cosh \varphi \alpha_i x + D_i \cosh \Phi \alpha_i x)$$

$$V_i(x) = (A_i \cosh \varphi \alpha_i x - \Phi B_i \cosh \Phi \alpha_i x) + (C_i \sinh \varphi \alpha_i x - \Phi D_i \sinh \Phi \alpha_i x)$$

Substitution of Eq. 42 into Eq. 40 and then into Eq. 37 yields:

$$n_x = \frac{E}{(1 + \nu)} \sum_{i=1}^{\infty} \left\{ - \left[1 - (1 + \nu) \epsilon \right] (A_i \cosh \varphi \alpha_i x + C_i \sinh \varphi \alpha_i y) + \Phi (B_i \cosh \Phi \alpha_i x + D_i \sinh \Phi \alpha_i x) \right\} \alpha_i \sin \alpha_i y \quad (43)$$

$$n_{xy} = \frac{E}{(1 + \nu)} \sum_{i=1}^{\infty} \left\{ \varphi(A_i \sinh \varphi \alpha_i x + C_i \cosh \varphi \alpha_i x) - [1 - (1 + \nu) \epsilon] \right. \\ \left. (B_i \sinh \bar{\varphi} \alpha_i x + D_i \cosh \bar{\varphi} \alpha_i x) \right\} \alpha_i \cos \alpha_i y$$

At this point, again, it is convenient to represent the forces and displacements of the panel edges by their symmetric and anti-symmetric components; that is,

$$\begin{aligned} N_i^s &= 1/2(N_i' + N_i) & N_i^{a/s} &= 1/2(N_i' - N_i) \\ T_i^s &= 1/2(T_i' + T_i) & T_i^{a/s} &= 1/2(T_i' - T_i) \\ U_i^s &= 1/2(U_i' + U_i) & U_i^{a/s} &= 1/2(U_i' - U_i) \\ V_i^s &= 1/2(V_i' + V_i) & V_i^{a/s} &= 1/2(V_i' - V_i) \end{aligned} \quad (44)$$

The panel edge forces can be found from Eqs. 43 and are defined as follows:

$$\begin{aligned} N_i &= n_x(-a/2) & T_i &= n_{xy}(-a/2) \\ N_i' &= n_x(a/2) & T_i' &= n_{xy}(a/2) \end{aligned} \quad (45)$$

The panel edge displacements are found in a similar way by use of Eqs. 42.

The following expressions for the symmetric and anti-symmetric components of the panel edge forces in terms of the symmetric and anti-symmetric panel edge displacements can be derived from Eq. 32:

$$\begin{aligned} N_i^s &= (b_{11} + b_{13})U_i^s + (b_{12} + b_{14})V_i^s \\ T_i^s &= (b_{12} + b_{14})U_i^s + (b_{22} + b_{24})V_i^s \end{aligned} \quad (46)$$

$$\begin{aligned} N_i^{a/s} &= (b_{11} - b_{13})U_i^{a/s} + (b_{12} - b_{14})V_i^{a/s} \\ T_i^{a/s} &= (b_{12} - b_{14})V_i^{a/s} + (b_{22} - b_{24})V_i^{a/s} \end{aligned} \quad (47)$$

1.2 Solution for Symmetric Case

The solution of $U_i(x)$, (Eq. 42), for this type of loads must be an even function of x and an odd function for $V_i(x)$. The constants of integration C_i and D_i are identically zero and only A_i and B_i have to be determined from the boundary conditions, Eq. 39. The general stresses are found from Eq. 43 which, together with Eqs. 44 and 45, yield expressions for N_i^s and T_i^s . Comparison with Eq. 46 then results in

$$\begin{aligned} (a/Et)(b_{11} + b_{13}) &= \frac{\epsilon \bar{\phi} \alpha_i a}{I^s} \cosh \frac{\varphi \alpha_i a}{2} \cosh \frac{\bar{\phi} \alpha_i a}{2} \\ (a/Et)(b_{22} + b_{24}) &= \frac{\epsilon \varphi \alpha_i a}{I^s} \sinh \frac{\varphi \alpha_i a}{2} \sinh \frac{\bar{\phi} \alpha_i a}{2} \end{aligned} \quad (48)$$

$$(a/Et)(b_{12} + b_{14}) = \frac{\epsilon \alpha_i a}{I^s} \cosh \frac{\varphi \alpha_i a}{2} \sinh \frac{\bar{\phi} \alpha_i a}{2} - \frac{\alpha_i a}{1 + \nu}$$

where
$$I^s = \cosh \frac{\varphi \alpha_i a}{2} \sinh \frac{\bar{\phi} \alpha_i a}{2} - \varphi \bar{\phi} \sinh \frac{\varphi \alpha_i a}{2} \cosh \frac{\bar{\phi} \alpha_i a}{2}$$

Expanding Eq. 48 in powers of ϵ and then investigating the eigenvalues of Eq. 46, that is, for

$$(b_{11} + b_{13})(b_{22} + b_{24}) - (b_{12} + b_{14})^2 = 0$$

Wittrick found that eigenvalues of ϵ always are of unit order, which implies that in practice the destabilizing effect of the stress σ in the symmetric mode of deformation is always insignificant. Therefore, only the leading terms of the expansion of Eq. 48 will be retained, which are as follows:

$$\begin{aligned} (a/Et)J^S(b_{11} + b_{13}) &= \frac{2\alpha_1 a}{1 + \nu} (\cosh \alpha_1 a + 1) \\ (a/Et)J^S(b_{22} + b_{24}) &= \frac{2\alpha_1 a}{1 + \nu} (\cosh \alpha_1 a - 1) \\ (a/Et)J^S(b_{12} + b_{14}) &= -\alpha_1 a \left(\frac{1 - \nu}{1 + \nu} \sinh \alpha_1 a - \alpha_1 a \right) \end{aligned} \quad (49)$$

where $J^S = (3 - \nu) \sinh \alpha_1 a - (1 + \nu) \alpha_1 a$

Eqs. 49 do not include the effect of the compressive stress σ anymore. They can be used to determine the stiffness matrix for a membrane without compressive stresses acting. Such a stiffness matrix has been found by Dean [12], and it can serve as one way to check the more complicated stiffness matrix obtained by Wittrick for the lower bound of σ .

1.3 Solution for Anti-Symmetric Case

The solution of $U_i(x)$, Eq. 42, for this type of loads must be an odd function of x and an even function for $V_i(x)$. The constants of integration A_i and B_i are identically zero and only C_i and D_i have to be determined from the boundary conditions, Eq. 39. Comparison of the resulting expressions for $N_i^{a/s}$ and $T_i^{a/s}$ with those of Eq. 47 yields

$$\begin{aligned}
(a/Et)(b_{11} - b_{13}) &= \frac{\epsilon \bar{\Phi} \alpha_1 a}{I a/s} \sinh \frac{\varphi \alpha_1 a}{2} \sinh \frac{\bar{\Phi} \alpha_1 a}{2} \\
(a/Et)(b_{22} - b_{24}) &= \frac{\epsilon \varphi \alpha_1 a}{I a/s} \cosh \frac{\varphi \alpha_1 a}{2} \cosh \frac{\bar{\Phi} \alpha_1 a}{2} \\
(a/Et)(b_{12} - b_{14}) &= \frac{\epsilon \alpha_1 a}{I a/s} \sinh \frac{\varphi \alpha_1 a}{2} \cosh \frac{\bar{\Phi} \alpha_1 a}{2} - \frac{\alpha_1 a}{1 + \nu}
\end{aligned} \tag{50}$$

$$\text{where } I a/s = \sinh \frac{\varphi \alpha_1 a}{2} \cosh \frac{\bar{\Phi} \alpha_1 a}{2} - \varphi \bar{\Phi} \cosh \frac{\varphi \alpha_1 a}{2} \sinh \frac{\bar{\Phi} \alpha_1 a}{2}$$

Expansion of Eqs. 50 in powers of ϵ and omitting the terms involving the compressive stress provides the second group of equations needed to determine the stiffness matrix for the membrane that is not in compression:

$$\begin{aligned}
(a/Et)J^{a/s}(b_{11} - b_{13}) &= \frac{2\alpha_1 a}{1 + \nu} (\cosh \alpha_1 a - 1) \\
(a/Et)J^{a/s}(b_{22} - b_{24}) &= \frac{2\alpha_1 a}{1 + \nu} (\cosh \alpha_1 a + 1) \\
(a/Et)J^{a/s}(b_{12} - b_{14}) &= -\alpha_1 a \left(\frac{1 - \nu}{1 + \nu} \sinh \alpha_1 a + \alpha_1 a \right)
\end{aligned} \tag{51}$$

$$\text{where } J^{a/s} = (3 - \nu) \sinh \alpha_1 a + (1 + \nu) \alpha_1 a$$

1.4 Stiffness Matrix

The total solution for the elements of the in-plane stiffness matrix can be assembled from Eqs. 48 and 50 which include the effects of the compressive stress σ :

$$\begin{aligned}
b_{11}, b_{13} &= \sigma t \alpha_1 \left(\frac{1}{I s} \cosh \varphi \alpha_1 a \cdot \cosh \bar{\Phi} \alpha_1 a \pm \frac{1}{I a/s} \sinh \varphi \alpha_1 a \cdot \sinh \bar{\Phi} \alpha_1 a \right) \\
b_{22}, b_{24} &= \sigma t \alpha_1 \left(\frac{1}{I s} \sinh \varphi \alpha_1 a \cdot \sinh \bar{\Phi} \alpha_1 a \pm \frac{1}{I a/s} \cosh \varphi \alpha_1 a \cdot \cosh \bar{\Phi} \alpha_1 a \right)
\end{aligned} \tag{52}$$

$$b_{14} = \sigma t \alpha_i \left(\frac{1}{I^s} \cosh \varphi \alpha_i a \cdot \sinh \Phi \alpha_i a - \frac{1}{I^{a/s}} \sinh \varphi \alpha_i a \cdot \cosh \Phi \alpha_i a \right)$$

$$b_{12} = \sigma t \alpha_i \left(\frac{1}{I^s} \cosh \varphi \alpha_i a \cdot \sinh \Phi \alpha_i a + \frac{1}{I^{a/s}} \sinh \varphi \alpha_i a \cdot \cosh \Phi \alpha_i a \right) - \frac{E t \alpha_i}{1 + \nu}$$

where I^s and $I^{a/s}$ are defined in Eqs. 48 and 50.

Eqs. 49 and 51, which do not include the effects of the compressive stress σ , can be used to find the following elements of the stiffness matrix of the classic plane stress analysis

$$b_{11}, b_{13} = \frac{E t \alpha_i}{1 + \nu} \left[\left(\frac{1}{J^s} (\cosh \alpha_i a + 1) \pm \frac{1}{J^{a/s}} (\cosh \alpha_i a - 1) \right) \right] \quad (53)$$

$$b_{22}, b_{24} = \frac{E t \alpha_i}{1 + \nu} \left[\left(\frac{1}{J^s} (\cosh \alpha_i a - 1) \pm \frac{1}{J^{a/s}} (\cosh \alpha_i a + 1) \right) \right]$$

$$b_{12}, b_{14} = - \frac{E t \alpha_i}{2} \left[\frac{1 - \nu}{1 + \nu} \sinh \alpha_i a \left(\frac{1}{J^s} \pm \frac{1}{J^{a/s}} \right) - \alpha_i a \left(\frac{1}{J^s} \mp \frac{1}{J^{a/s}} \right) \right]$$

where J^a and $J^{a/s}$ are defined in Eqs. 49 and 51.

It can be shown that Eqs. 53 are identical to the corresponding equations derived by Dean.

This completes the derivation of the boundary force-deformation relations for the Composite Membrane Analysis.

For convenience in the derivation of the buckling criteria for the ribbed membrane, the orientation of the positive direction of $T'(y)$ and $V'(y)$ will be reversed. This results in the change of sign of the expressions for b_{12} and b_{24} in Eqs. 52 and 53 and in the following modification of Eq. 32:

$$\begin{Bmatrix} N \\ T \\ N' \\ T' \end{Bmatrix}_i = \begin{bmatrix} -b_{11} & b_{12} & b_{13} & -b_{14} \\ b_{12} & -b_{22} & b_{14} & b_{24} \\ -b_{13} & -b_{14} & b_{11} & b_{12} \\ b_{14} & -b_{24} & b_{12} & b_{22} \end{bmatrix} \begin{Bmatrix} U \\ V \\ U' \\ V' \end{Bmatrix}_i \quad (54)$$

The stiffeners can be considered as beams using the assumptions of engineering theory. The governing differential equation for a beam under in-plane loads is derived in the appendix.

An alternate solution is obtained by considering the ribs as flat strips with one free edge, that is by setting $N_i' = T_i' = 0$ in Eq. 54 and solving for N_i and T_i in terms of U_i and V_i alone. The modified Eq. 54 is found by subdividing the coefficient matrix and has the following form:

$$\begin{Bmatrix} N_i \\ T_i \end{Bmatrix} = \begin{bmatrix} c_{11} & c_{12} \\ c_{12} & c_{22} \end{bmatrix} \begin{Bmatrix} U_i \\ V_i \end{Bmatrix} \quad (55)$$

where

$$\begin{bmatrix} c_{11} & c_{12} \\ c_{12} & c_{22} \end{bmatrix} = \begin{bmatrix} -b_{11} & b_{12} \\ b_{12} & -b_{22} \end{bmatrix} - \begin{bmatrix} b_{13} & -b_{14} \\ b_{14} & b_{24} \end{bmatrix} \begin{bmatrix} b_{11} & b_{12} \\ b_{12} & b_{22} \end{bmatrix}^{-1} \begin{bmatrix} -b_{13} & -b_{14} \\ b_{14} & -b_{24} \end{bmatrix}$$

To distinguish between membrane and rib quantities, the terms involving rib quantities will be barred whenever they are used hereafter.

2. Derivation of the Buckling Criteria

2.1 Equilibrium Equations

This derivation for the Membrane Analysis follows the very same steps as did the derivation for the Flexural Analysis. A less detailed presentation is therefore outlined in this chapter.

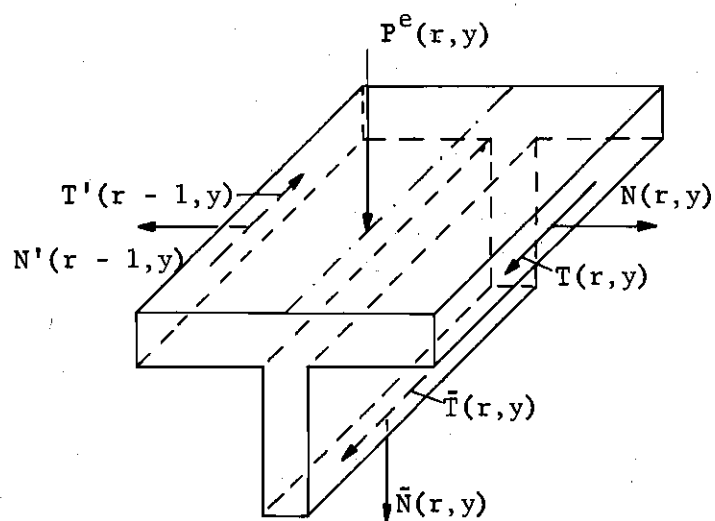
The three equations of equilibrium for a rib line element (Fig. 12) for the Composite Membrane Analysis are:

$$\begin{aligned} N(r,y) - N'(r-1,y) &= 0 \\ T(r,y) - T'(r-1,y) + \bar{T}(r,y) &= 0 \\ \bar{N}(r,y) + P^e(r,y) &= 0 \end{aligned} \tag{56}$$

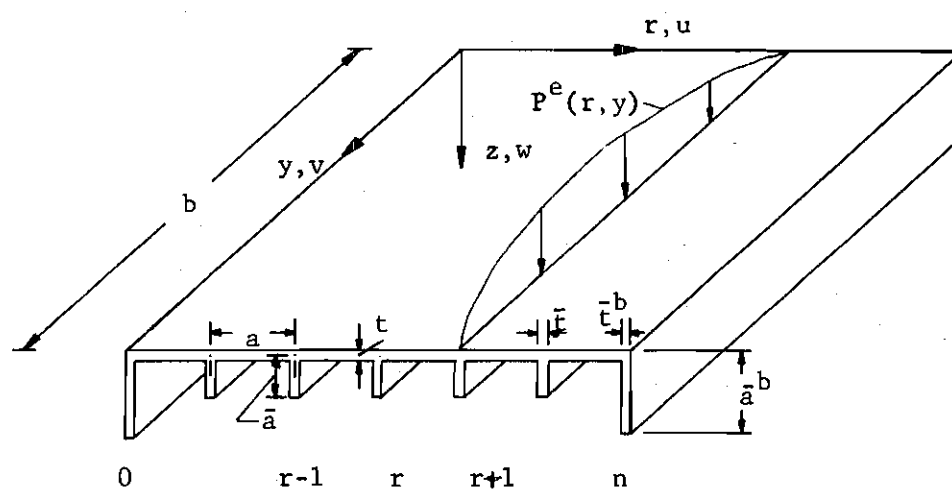
Here $N(r,y)$, $N'(r,y)$, $T(r,y)$, and $T'(r,y)$ are the membrane boundary forces on the typical panel r , between the rib lines r and $r+1$. They are defined below in a manner analogous to Eq. 10:

$$\begin{aligned} \begin{Bmatrix} N(r,y) \\ N'(r,y) \end{Bmatrix} &= \sum_{i=1}^{\infty} \begin{Bmatrix} N(r) \\ N'(r) \end{Bmatrix} \sin \alpha_i y \\ \begin{Bmatrix} T(r,y) \\ T'(r,y) \end{Bmatrix} &= \sum_{i=1}^{\infty} \begin{Bmatrix} T(r) \\ T'(r) \end{Bmatrix} \cos \alpha_i y \end{aligned} \tag{57}$$

$\bar{N}(r,y)$ and $\bar{T}(r,y)$ are the direct and shear forces acting along the top of the rib r . For simple support conditions at the ends (see Eq. 39), these line or membrane forces also can be expanded into infinite series of the same form as Eq. 57. The equivalent line loads $P^e(r,y)$ are expressed in series form in Eq. 14. Replacement of all quantities in Eqs. 56 by their equivalent series and matching like coefficients results



(a) Rib Line Element



(b) Rib and Membrane System

Figure 14. Composite Membrane Model

in the following relations between the series coefficients:

$$N_i(r) - N_i'(r - 1) = 0 \quad (58)$$

$$T_i(r) - T_i'(r - 1) + \bar{T}_i(r) = 0$$

$$\bar{N}_i(r) + P_i(r) = 0$$

2.2 Displacements

The membrane force coefficients in these equations can be expressed in terms of the coefficients of the in-plane panel boundary displacements by use of the membrane stiffness coefficients shown in Eq. 54. Similarly, the coefficients of the line forces on the ribs can be expressed in terms of the coefficients of the y and z components of the rib line displacements. Since the ribs are considered as flat strips, Eq. 55 gives the desired relationships. The in-plane panel boundary displacements are as follows:

$$\frac{1}{a} \begin{Bmatrix} u(-a/2, r, y) \\ u(a/2, r, y) \end{Bmatrix} = \begin{Bmatrix} U(r, y) \\ U'(r, y) \end{Bmatrix} = \sum_{i=1} \begin{Bmatrix} U_i(r) \\ U_i'(r) \end{Bmatrix} \sin \alpha_i y$$

$$\frac{1}{a} \begin{Bmatrix} v(-a/2, r, y) \\ v(a/2, r, y) \end{Bmatrix} = \begin{Bmatrix} V(r, y) \\ V'(r, y) \end{Bmatrix} = \sum_{i=1} \begin{Bmatrix} V_i(r) \\ V_i'(r) \end{Bmatrix} \cos \alpha_i y$$

Consideration of displacement compatibility and continuity at the rib lines yields the following expressions:

$$aV_i(r) = \bar{a}\bar{V}_i(r) \quad U_i'(r - 1) = U_i(r)$$

$$aW_i(r) = \bar{a}\bar{U}_i(r) \quad V_i'(r - 1) = V_i(r)$$

2.3 Governing Difference Equations for the Rib Line Displacements

Substitution of the compatibility, continuity, and force-deformation relations into Eqs. 58 results in three difference equations for the coefficients of the rib line displacements. After eliminating $W_i(r)$, the following two uncoupled difference equations for the simply supported stiffened membrane result:

$$\begin{bmatrix} b_{13}(\nabla_r - 2\gamma_i) & -2b_{14}\bar{\nabla}_r \\ 2b_{14}\bar{\nabla}_r & b_{24}(\nabla_r - 2\bar{\gamma}_i) \end{bmatrix} \begin{bmatrix} U_i(r) \\ V_i(r) \end{bmatrix} = \begin{bmatrix} 0 \\ \bar{P}_i(r) \end{bmatrix} \quad (59)$$

where ∇_r and $\bar{\nabla}_r$ are defined in Eq. 18.

$$\gamma_i = b_{11}/b_{13} - 1$$

$$\bar{\gamma}_i = b_{22}/b_{24} - 1 - (a/2\bar{a}) \frac{\bar{c}_{12}^2 - \bar{c}_{11}\bar{c}_{22}}{b_{24}\bar{c}_{11}}$$

and

$$\bar{P}_i(r) = (\bar{c}_{12}/\bar{c}_{11})P_i(r)$$

This equation can be used to find the rib line displacements for low loads. Here it will be used to find the buckling criteria for initial buckling for the Composite Membrane Model.

Note that the signs of b_{12} and b_{24} have been changed from their original definition in Eq. 52 and that the barred quantities \bar{c}_{11} to \bar{c}_{22} are derived from Eq. 55 with the flat strip properties and, if applicable, the rib stress $\bar{\sigma}$ replacing the membrane properties and the stress σ .

3. Simple Side Supports

The series coefficients of Eq. 59 can be expanded into finite series in r for this case just as in Chapter II. In analogy to Eq. 22, these coefficients will be expressed as follows,

$$\begin{aligned} \begin{Bmatrix} V_i(r) \\ W_i(r) \\ \bar{P}_i(r) \end{Bmatrix} &= \sum_{k=1}^{n-1} \begin{Bmatrix} V_{ik} \\ W_{ik} \\ \bar{P}_{ik} \end{Bmatrix} \cdot \sin \frac{k\pi r}{n} \\ U_i(r) &= \sum_{k=0}^n U_{ik} \cos \frac{k\pi r}{n} \end{aligned} \quad (60)$$

Substitution of Eq. 60 into Eq. 59 and solving for the in-plane displacement coefficients in terms of the loading coefficients yields:

$$\begin{bmatrix} b_{13}(\gamma_i + \sigma_k) & b_{14} \sin \frac{k\pi}{n} \\ b_{14} \sin \frac{k\pi}{n} & b_{24}(\bar{\gamma}_i + \sigma_k) \end{bmatrix} \begin{Bmatrix} U_{ik} \\ V_{ik} \end{Bmatrix} = \begin{Bmatrix} 0 \\ -\frac{1}{2} \bar{P}_{ik} \end{Bmatrix} \quad (61)$$

in which σ_k is defined in Eq. 23.

Solving this equation for U_{ik} and V_{ik} yields

$$\begin{aligned} U_{ik} &= \frac{\frac{1}{2} b_{14} \sin \frac{k\pi}{n} \bar{P}_{ik}}{|c_{ik}|} \\ V_{ik} &= \frac{-\frac{1}{2} b_{13}(\gamma_i + \sigma_k)}{c_{ik}} \bar{P}_{ik} \end{aligned} \quad (62)$$

in which

$$|c_{ik}| = b_{13} b_{24} (\gamma_i + \sigma_k) (\bar{\gamma}_i + \sigma_k) - b_{14}^2 \sigma_k (2 - \sigma_k)$$

The coefficients of the out-of-plane displacements can be found from the third of Eqs. 58. Substitution of the compatibility and force-deformation relations into this equation yields

$$\bar{c}_{12} V_i(r) + \bar{c}_{11} W_i(r) = \frac{\bar{a}}{a} P_i(r)$$

from which W_{ik} is obtained as follows

$$W_{ik} = \frac{\bar{c}_{12}}{\bar{c}_{11}} V_{ik} - \frac{\bar{a}\bar{P}_{ik}}{a\bar{c}_{12}} \quad (63)$$

Eqs. 62 and 63 comprise the solution for the coefficients of the rib line displacements of a ribbed membrane that is simply supported on all four edges of the boundary with specified rib line loading coefficients, P_{ik} or \bar{P}_{ik} .

4. Buckling with Simple Side Supports

Eq. 61 has non-trivial solutions for zero external loads, $P_{ik} = 0$, only for a vanishing determinant of coefficients, that is for $C_{ik} = 0$. The buckling criterion, therefore, is $C_{ik} = 0$ and it is utilized in exactly the same way for the ribbed membrane as was the criterion $C_{ik}' = 0$ for the flexural ribbed plate. Setting the rib dimensions and properties equal to zero yields one limiting case of an unstiffened membrane. On the other hand, the limit would be a system of flat strips in compression, not connected by a membrane. This would yield the analogy to the simple column case, the buckling of flat strips having two free sides.

For the first limiting case, the unstiffened membrane, Eqs. 50 can be used to find the lowest eigenvalue that satisfies the buckling criterion. It has been noted that in the symmetric mode for the loads and displacements,

σ has no destabilizing effect. Therefore, it is sufficient only to investigate the results of the anti-symmetric mode, that is Eqs. 50. The eigenvalues must satisfy the condition (see Eq. 47),

$$(b_{11} - b_{13})(b_{22} - b_{24}) - (b_{12} - b_{14})^2 = 0$$

Substituting the expanded Eqs. 50 without omitting the terms involving the compressive stress (see Page) into this equation and retaining only the lowest powers of ϵ and α_i , Wittrick found that

$$\epsilon_{cr} = \frac{a^2 \alpha_i^2}{12} \quad \text{or} \quad \sigma_{cr} = \frac{i^2 \pi^2 E a^2}{12 b^2}$$

which is the stress given by the Euler formula for buckling in the plane of the membrane with a half-wave length of b/i .

In order to get an idea of the range of applicability of the in-plane buckling criteria for a single panel, the above formula will now be compared to the formula given for the out-of-plane buckling stress. The critical in-plane stress attains its highest values for $i = 1$; that is, for buckling in one longitudinal half-wave. Setting the aspect ratio b/a equal to λ , the above formula becomes, for $i = 1$,

$$\sigma_{cr}^{in} = \frac{\pi^2 E}{12 \lambda^2}$$

The critical out-of-plane stresses for the single panel, as stated in the Introduction, were found to be

$$\sigma_{cr}^{out} = k_{cr} \frac{\pi^2 E t^2}{12(1-\nu^2)a^2}$$

where k_{cr} is known to have a smallest value of 4 for buckling into squares. Setting the slenderness ratio a/t equal to β , this equation becomes, for $k_{cr} = 4$,

$$\sigma_{cr}^{out} = \frac{4 \pi^2 E}{12(1-\nu^2) \beta^2}$$

Comparison of σ_{cr}^{in} and σ_{cr}^{out} shows that these two critical stresses are approximately equal for $\beta = 2\lambda$, that is, for very narrow and thick plates. For all practical cases, however, the plate will buckle out-of-plane long before the critical stress for in-plane buckling is reached. The boundary conditions encountered in most cases are such as to favor out-of-plane buckling over in-plane buckling. Additional constraints against the previous would be necessary if the latter should govern. For a numerical comparison set $\lambda = 10$, $\beta = 50$, $E = 29000$ ksi, $\nu = 0.3$, $i = 1$, $k_{cr} = 4$, then

$$\sigma_{cr}^{in} = 238 \text{ ksi}$$

$$\sigma_{cr}^{out} = 42 \text{ ksi}$$

5. Boundary Deflections

The second solution of the Composite Membrane Analysis for a ribbed membrane is for the unloaded system, $P_{ik} = 0$, with inhomogeneous conditions along two sides of the boundary, that is, with imposed boundary deflections V_i at $r = 0$ and $r = n$. V_i is represented by its symmetric and anti-symmetric components, that is by

$$V_i^s = 1/2[V_i(0) + V_i(n)] \quad V_i^{a/s} = 1/2[V_i(0) - V_i(n)]$$

Including corrective terms, the Fourier series expansions for the symmetric components of the displacement coefficients in Eq. 59 can be written in the following form

$$\bar{v}_i^s(r) = v_i^s \left(1 + \sum_{k=1,3,\dots}^{n-1} \bar{v}_{ik} \sin \frac{k\pi r}{n} \right) \quad (64)$$

$$\bar{u}_i^s(r) = v_i^s \sum_{k=1,3,\dots}^n \bar{u}_{ik} \cos \frac{k\pi r}{n}$$

Substitution of Eqs. 64 into the governing differential equation 59 and into the boundary conditions yields

$$\bar{u}_{ik} = \frac{2b_{24}\varphi_k}{n|c_{ik}|} (b_{14}\bar{v}_i(2 - \sigma_k) - (b_{14} - b_{12})(\bar{v}_i + \sigma_k))$$

$$\bar{v}_{ik} = \frac{2(2 - \sigma_k)}{n \sin \frac{k\pi}{n} |c_{ik}|} [b_{14}(b_{14} - b_{12})\sigma_k - b_{13}b_{24}\bar{v}_i(\bar{v}_i + \sigma_k)]$$

where φ_k is defined in analogy to Eq. 22 as $\varphi_k = \begin{cases} 1 & \text{for } k = 1, (1), n-1 \\ 1/2 & \text{for } k = 0, n \end{cases}$

For the anti-symmetric components, the solution can be written in the following form

$$\bar{v}_i^{a/s} = v_i^{a/s} \left[\left(1 - \frac{2r}{n} \right) + \sum_{k=2,4,\dots}^{n-1} \bar{v}_{ik} \sin \frac{k\pi r}{n} \right] \quad (65)$$

$$\bar{u}_i^{a/s} = v_i^{a/s} \sum_{k=0,2,\dots}^n \bar{u}_{ik} \cos \frac{k\pi r}{n}$$

where \bar{v}_{ik} and \bar{u}_{ik} are identical to the ones for the symmetric case.

6. Rib Boundary

The total solution for the Composite Membrane Analysis of a ribbed plate is that for a composite boundary rib or beam. It can be obtained by superposition of the results given in Eqs. 60, 64, and 65 and is shown in Eq. 66:

$$V_i^t(r) = V_i(r) + \bar{V}_i^s(r) + \bar{V}_i^{a/s}(r) \quad (66)$$

$$U_i^t(r) = U_i(r) + \bar{U}_i^s(r) + \bar{U}_i^{a/s}(r)$$

Again, as in the Flexural Analysis, the interior ribs may or may not be equal to the boundary ribs and the two boundary ribs are chosen to be identical, so that the structure is symmetric about $r = n/2$. The coefficients V_i^s and $V_i^{a/s}$ are obtained by satisfying the last two of Eqs. 58.

They can be obtained separately by working with the symmetric and anti-symmetric loading components, corresponding to k odd and k even respectively. These loading components are the same as in Eq. 29.

The last two of Eqs. 58 in terms of the boundary rib displacements result in the following condition:

$$b_{14}(\Delta_r + \epsilon_i^b)U_i^t(0) + b_{24}(\Delta_r - \bar{\gamma}_i^b)V_i^t(0) = \bar{p}_i^s \quad (67)$$

in which

$$\epsilon_i^b = \frac{b_{14} + b_{12}}{b_{14}}$$

$$\bar{\gamma}_i^b = \bar{\epsilon}_i^b + \frac{a}{b_{24}\bar{a}^b} \left[\frac{\bar{c}_{12}^2 - \bar{c}_{11}\bar{c}_{22}}{\bar{c}_{11}} \right]^b$$

$$\bar{\epsilon}_i^b = \frac{b_{22} - b_{24}}{b_{24}}$$

$$\bar{p}_i^s = \left[\frac{\bar{c}_{12}}{\bar{c}_{11}} \right]^b \cdot p_i^s$$

Δ_r is defined in Eq. 21

Substitution of Eq. 66 into Eq. 67 and solving for V_i^s yields

$$V_i^s = \frac{\bar{p}_i^s - t_i^s(0)}{\bar{t}_i^s(0) + b_{24}(\bar{\epsilon}_i - \bar{\gamma}_i)^b} = \frac{\bar{p}_i^s - t_i^s(0)}{\bar{t}_i^s(0) - \eta_i^b}$$

in which

$$\eta_i^b = a \cdot \left[\frac{\bar{c}_{12}^2 - \bar{c}_{11}\bar{c}_{22}}{\bar{c}_{11}\bar{a}} \right]^b$$

and $t_i^s(0)$ is the coefficient of the membrane boundary shear for the symmetrically loaded system with simple side supports and $\bar{t}_i^s(0)$ is the coefficient of the membrane boundary shear for the symmetrical unit boundary deflection coefficient V_i^s , that is

$$t_i^s(0) = b_{14} \sum_{k=1,3,\dots}^n (\epsilon_i^b - \sigma_k) \bar{u}_{ik} + b_{24} \sum_{k=1,3,\dots}^{n-1} \bar{v}_{ik} \sin \frac{k\pi}{n}$$

$$\bar{t}_i^s(0) = b_{14} \sum_{k=1,3,\dots}^n (\epsilon_i^b - \sigma_k) \bar{u}_{ik} + b_{24} \left(\sum_{k=1,3,\dots}^{n-1} \bar{v}_{ik} \sin \frac{k\pi}{n} - \bar{\epsilon}_i^b \right)$$

The anti-symmetric component of the boundary deflection is obtained in a similar way as the symmetric component and is found to be

$$v_i^{a/s} = \frac{\bar{p}_i^{a/s} - t_i^{a/s}(0)}{\bar{t}_i^{a/s}(0) - \eta_i^b}$$

where η_i^b is defined as in the symmetric case and

$$t_i^{a/s}(0) = b_{14} \sum_{k=0,2,\dots}^n (\epsilon_i^b - \sigma_k) \bar{u}_{ik} + b_{24} \sum_{k=2,4,\dots}^{n-1} \bar{v}_{ik} \sin \frac{k\pi}{n}$$

$$\bar{t}_i^{a/s}(0) = b_{14} \sum_{k=0,2,\dots}^n (\epsilon_i^b - \sigma_k) \bar{u}_{ik} + b_{24} \left(\sum_{k=2,4,\dots}^{n-1} \bar{v}_{ik} \sin \frac{k\pi}{n} - \bar{\epsilon}_i^b - \frac{2}{n} \right)$$

This completes the solution of the deflections of a ribbed plate with beam boundaries subject to transverse and in-plane compressive loads and using a Composite Flexural Analysis.

7. Buckling with Rib Boundaries

The criteria for the initial buckling of the ribbed membrane with beam boundaries follow in an exactly similar way to those for the ribbed plate. They take the following form:

$$c_{ik} = 0 \quad \bar{t}_i^s(0) - \eta_i^b = 0 \quad \bar{t}_i^{a/s} - \eta_i^b = 0$$

IV. CONCLUSIONS

Closed form solutions were obtained for the elastic analysis of deflections and the initial buckling for rectangular ribbed plates and membranes. The results are based on two rationally formulated discrete-continuous models of the fourth order. The only assumptions made were those associated with membrane or flexural plate theory and ordinary beam theory. In the Non-Composite Flexural Model, the structure is proportioned so that the effects of the in-plane plate deformations and T-beam action can be ignored in determining the stiffness matrix that relates the out-of-plane edge forces and the in-plane compressive stresses to the edge deformations. In the Composite Flexural Model, the effects of the out-of-plane deformations can be ignored. The techniques used permit the realistic treatment of simply supported plates as well as of plates having side boundary conditions other than simple supports. The results show the way for improved analysis of composite members, orthotropic panels, and multi-web beams.

A major advantage of the discrete-continuous approach is that simple equations for determining of the buckling criteria are obtained which are independent of the number of ribs. This number, as well as all the other pertinent data, is inserted directly into these equations that contain all possible buckling modes. The eigenvalues have to be found for one or two independent equations only and not for a system of equations, the size of which depends directly on the number of ribs, as in earlier solutions of the problem. This facilitates the use and application of these results

and makes them economic and attractively simple. Numerical examples show the usefulness of the techniques. They were obtained by using a high speed digital computer.

The stability equations can easily be used to generate curves or tables that show limiting values for rib-to-plate stiffness ratios that cause local buckling to govern as against system buckling. For given stiffnesses the limiting values for the rib spacing can be found.

The two fourth order models could be combined into an eighth order model, which is recommended as one extension of this thesis. The eighth order model could then be used to find the applicable range of validity for the solutions to the lower order models by comparison of the results. Another extension of this thesis would be the analysis of other ribbed structures such as ribbed cylindrical and other shells. The basic tool, the discrete-continuous approach, can be used for many types of structures.

APPENDIX

APPENDIX

1. Governing Differential EquationFor A Beam Under Out-of-Plane Loads

The governing differential equation is derived for a beam under eccentric lateral loads, $\bar{S}(y)$, and distributed lateral moments, $\bar{M}(y)$, in addition to a constant compressive load P (Fig. 15).

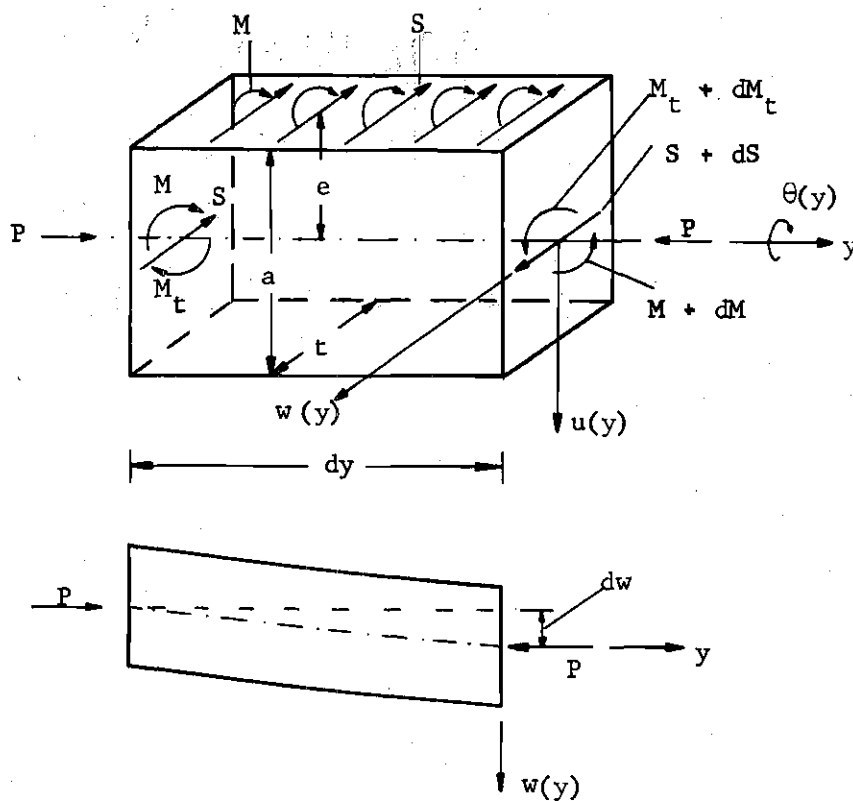


Figure 15. Beam Element with Applied Lateral Loads and Moments and Axial Force.

The three equations of equilibrium are

$$\Sigma F_v = 0 \quad \text{or} \quad D_y S = \bar{S}(y) \quad (68)$$

$$\Sigma M = 0 \quad \text{or} \quad D_y M = S + P D_y w \quad (69)$$

$$\Sigma M_t = 0 \quad \text{or} \quad D_y M_t = \bar{M}(y) + \bar{S}(y)e \quad (70)$$

Differentiating Eq. 69 and combination of the result with Eq. 68 yields

$$D_y^2 M = \bar{S}(y) + P D_y^2 w \quad (71)$$

Elementary beam bending theory provides $D_y^2 M = -EI_w D_y^2 w$ which, after combination with Eq. 71 yields

$$\bar{S}(y) = -B' D_y^4 w - P D_y^2 w = -(B' D_y^2 + P) D_y^2 w \quad (72)$$

where $B' = EI$ is the flexural rigidity of the beam about the x axis.

Elementary beam torsion theory provides $\bar{M}(y) + \bar{S}(y) = -GJ \cdot D_y^2 \theta$, where GJ is the torsional stiffness of the beam. Combination of this equation with (72) and introducing $\bar{k}B' = GJ$ yields

$$\bar{M}(y) = B' \left[-\bar{k} D_y^2 \theta + e(D_y^2 + \frac{P}{B'}) D_y^2 w \right] \quad (73)$$

Transformation of the w axis (see Fig. 16), and using W as for the panel deflections, that is

$$W(y) = \frac{1}{a} w(-\frac{a}{2}, y) = \frac{1}{a} [w(y) - e\theta(y)]$$

or

$$w(y) = aW(y) + e\theta(y)$$

yields, after introducing into Eqs. 72 and 73, and arranging in matrix notation

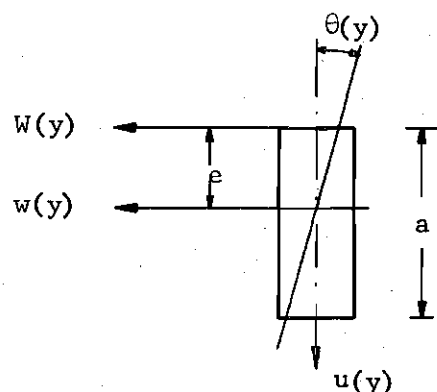


Figure 16. Transformation of the W-Axis of the Beam.

$$B' \begin{bmatrix} e^2 D_y^4 + \frac{P}{B'} D_y^2 - \bar{k} D_y^2 & e a (D_y^4 + \frac{P}{B'} D_y^2) \\ -e (D_y^4 + \frac{P}{B'} D_y^2) & -a (D_y^4 + \frac{P}{B'} D_y^2) \end{bmatrix} \begin{bmatrix} \theta(y) \\ W(y) \end{bmatrix} = \begin{bmatrix} \bar{M}(y) \\ \bar{S}(y) \end{bmatrix} \quad (74)$$

which is the sought governing differential equation for the beam. Substitution of the series in Eqs. 9 and 10, repeated here for convenience

$$\begin{bmatrix} \theta(r,y) \\ W(r,y) \\ \bar{M}(r,y) \\ \bar{S}(r,y) \end{bmatrix} = \sum_{i=1}^{\infty} \begin{bmatrix} \theta_i(r) \\ W_i(r) \\ \bar{M}_i(r) \\ \bar{S}_i(r) \end{bmatrix} \sin \alpha_i y \quad \alpha_i = \frac{i\pi}{b} \quad (9,10)$$

into Eq. 74 and matching like coefficients, yields

$$\alpha_i^2 B' \begin{bmatrix} e^2 (\alpha_i^2 - \frac{P}{B'}) + \bar{k} & e (\alpha_i^2 - \frac{P}{B'}) \\ -e (\alpha_i^2 - \frac{P}{B'}) & - (\alpha_i^2 - \frac{P}{B'}) \end{bmatrix} \begin{bmatrix} \theta_i(r) \\ W_i(r) \end{bmatrix} = \begin{bmatrix} \bar{M}_i(r) \\ \bar{S}_i(r) \end{bmatrix} \quad (75)$$

which is the governing differential equation for the beam expressed in terms of the Euler coefficients.

For $\bar{S}_i(r) = 0$, Eq. 75 can be solved for $\bar{M}_i(r)$ in terms of $\theta_i(r)$ and one obtains

$$\bar{M}_i(r) = \alpha_i^2 k_B' \theta_i(r) \quad (76)$$

2. Governing Differential Equation

For A Beam Under In-Plane Loads

The governing differential equation is derived for a beam under eccentric longitudinal loads, $\bar{T}(y)$, and transverse loads, $\bar{N}(y)$, in addition to a constant compressive axial load P (Fig. 17).

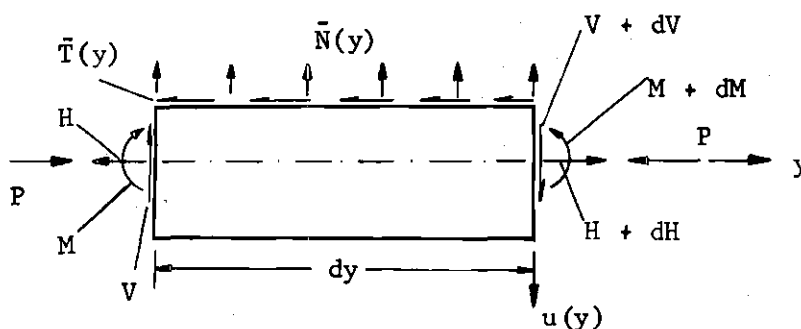


Figure 17. Beam Element with Applied Loads and Axial Force.

The three equilibrium equations are

$$\Sigma V = 0 \quad \text{or} \quad \frac{D}{Dy} V = \bar{N}(y) \quad (77)$$

$$\Sigma H = 0 \quad \text{or} \quad \frac{D}{Dy} H = \bar{T}(y) \quad (78)$$

$$\Sigma M = 0 \quad \text{or} \quad \frac{D}{Dy} M = V(y) + P \frac{D}{Dy} u - \bar{T}(y)e \quad (79)$$

Differentiating Eq. 79 and combining the result with Eq. 77 yields

$$\frac{D^2}{Dy^2} M = \frac{D}{Dy} V + P \frac{D^2}{Dy^2} u - e \frac{D}{Dy} \bar{T}(y) = \bar{N}(y) + P \frac{D^2}{Dy^2} u - e \frac{D}{Dy} \bar{T}(y) \quad (80)$$

Differentiating Eq. 78 and combination with Eq. 80 yields

$$D_y^2 M = \bar{N}(y) + PD_y^2 u - eD_y^2 H \quad (81)$$

From elementary beam bending theory, one obtains $D_y^2 M = -BD_y^4 u$ where B is the flexural rigidity of the beam about the w axis. Combination of this equation with Eq. 81 yields

$$-BD_y^4 u = \bar{N}(y) + PD_y^2 u - eD_y^2 H \quad (82)$$

The longitudinal stress at the top of the beam can be expressed as

$$\sigma_y = \frac{H - P}{A} - \frac{M}{I}e = \epsilon_y E = D_y v E$$

where A is the cross sectional area of the beam and E is the modulus of elasticity. Solving for H and setting $M = -BD_y^2 u$ yields

$$H = AED_y v + P - eAED_y^2 u$$

$$D_y H = AED_y^2 v - eAED_y^3 u \quad (83)$$

$$D_y^2 H = AED_y^4 u \quad (84)$$

Combining Eqs. 82 and 84 and noting that $I = Ar^2$, where r is the radius of gyration of the cross section of the beam with respect to the bending about the w axis, yields

$$\bar{N}(y) = -EA(r^2 + e^2)D_y^4 u - \frac{P}{EA}D_y^2 u + eD_y^3 v$$

Combining Eqs. 78 and 83 yields

$$\bar{T}(y) = -EA eD_y^3 u - D_y^2 v$$

In matrix notation, setting $U(y) = (1/a)u(-a/2, y)$ and $V(y) = (1/a)v(-a/2, y)$ as for the panel deflections, these equations can be expressed as follows:

$$aEA \begin{bmatrix} -(r^2 + e^2)D_y^4 - \frac{P}{EA} D_y^2 & eD_y^3 \\ eD_y^3 & -D_y^2 \end{bmatrix} \begin{bmatrix} U(y) \\ V(y) \end{bmatrix} = \begin{bmatrix} \bar{N}(y) \\ -\bar{T}(y) \end{bmatrix} \quad (85)$$

which is the sought governing differential equation of the beam.

Substitution of the series in Eqs. 57, repeated here for convenience,

$$\begin{bmatrix} U(r, y) \\ N(r, y) \end{bmatrix} = \sum_{i=1}^{\infty} \begin{bmatrix} U_i(r) \\ \bar{N}_i(r) \end{bmatrix} \sin \alpha_i y$$

$$\begin{bmatrix} V(r, y) \\ T(r, y) \end{bmatrix} = \sum_{i=0}^{\infty} \begin{bmatrix} U_i(r) \\ \bar{T}_i(r) \end{bmatrix} \cos \alpha_i y \quad (57)$$

into Eq. 85 and matching like coefficients yields

$$\alpha_i^2 aEA \begin{bmatrix} -(r^2 + e^2)\alpha_i^2 + \frac{P}{EA} & e\alpha_i \\ e\alpha_i & -1 \end{bmatrix} \begin{bmatrix} U_i(r) \\ V_i(r) \end{bmatrix} = \begin{bmatrix} \bar{N}_i(r) \\ \bar{T}_i(r) \end{bmatrix} \quad (86)$$

which is the governing differential equation of the beam expressed in terms of the Euler coefficients.

For $\bar{T}_i(r) = 0$, Eq. 86 can be solved for $\bar{N}_i(r)$ in terms of $U_i(r)$ and one obtains

$$\bar{N}_i(r) = a\alpha_i^2 (P - \alpha_i^2 B) U_i(r) \quad (87)$$

BIBLIOGRAPHY

1. Timoshenko, S. P., and Gere, J. M., Theory of Elastic Stability, McGraw Hill Book Co., Inc., New York, 2nd Edition, 1961
2. Girkmann, Karl, Flächentragwerke, Springer Verlag, Wien, 5. Auflage, 1959
3. Bryan, G. H., "Buckling of Compressed Plates," Proc. of the London Mathematical Society, Vol. 12, p. 54, 1891
4. Rendulic, L., "Über die Stabilität von Stäben welche aus einem mit Randwinkeln verstärkten Bleche bestehen," Ingenieur-Archiv, Vol. 3, p. 447, 1932
5. Chwalla, E., "Das allgemeine Stabilitätsproblem der gedrückten, durch Randwinkel verstärkten Platte," Ingenieur-Archiv, Vol. 5, p. 54, 1934
6. Miles, A. J., "Stability of Rectangular Plates Elastically Supported at the Edges," Journal of Applied Mechanics, Vol. 3, p. A-47, 1936
7. Barbré, R., Stabilität gleichmässig gedrückter Rechteckplatten mit Längs- und Quersteifen," Ingenieur-Archiv, Vol. 8, p. 117, 1937
8. Bleich, Friedrich, Buckling Strength of Metal Structures, McGraw Hill Book Co., Inc., New York, 1952
9. Wittrick, W. H., "A Unified Approach to the Initial Buckling of Stiffened Panels in Compression," The Aeronautical Quarterly, Vol. 19, p. 265, August, 1968
10. Pflüger, Alf, "Zum Beulproblem der anisotropen Rechteckplatte," Ingenieur-Archiv, Vol. 16, p. 111, 1947
11. Kapur, K. K., and Hartz, B. J., "Stability of Plates Using the Finite Element Method," Journal of The Engineering Mechanics Div., ASCE, Vol. 92, No. EM2, p. 177, April 1966
12. Dean, D. L., "Analysis of Ribbed Plates," Highway Research Program, School of Engineering, North Carolina State University, Project ERD-110-67-4
13. Novozhilov, V. V., Foundations of the Non-Linear Theory of Elasticity," Graylock Press, Rochester, N.Y., 1953, translated from the first Russian edition, 1948
14. Lokshin, A. S., "On the Calculation of Plates with Ribs," Journal of Applied Mathematics and Mechanics, 1st Series, Moscow, Vol. 2, p. 225, 1935

15. Klöppel, K. and Scheer, J., Beulwerte ausgesteifter Rechteckplatten, Vol. 1, Wilhelm Ernst u. Sohn, Berlin, 1960
16. Klöppel, K. and Möller, K. H., Beulwerte ausgesteifter Rechteckplatten, Vol. 2, Wilhelm Ernst u. Sohn, Berlin, 1968
17. Stiffel, Rudolf, "Biegungsbeulung versteifter Rechteckplatten," Der Bauingenieur, Vol. 22, p. 367, October 1944
18. Brockenbrough, R. L. and Johnston, B. G. USS Steel Design Manual, United States Steel Corp. ADUSS 27-3400-02, November 1968